

TRANSFER FUNCTION INTERPOLATION REMAINDER FORMULA OF RATIONAL KRYLOV SUBSPACE METHODS*

YIDING LIN[†]

Abstract. Rational Krylov subspace projection methods have proven to be a highly successful approach in the field of model order reduction (MOR), primarily due to the fact that some derivatives of the approximate and original transfer functions are identical. This is the well-known theory of moments matching. Nevertheless, the properties of points situated at considerable distances from the interpolation nodes remain underexplored. In this paper, we present the explicit expression of the MOR error, which involves both the shifts and the Ritz values. The superiority of our discoveries over the known moments matching theory can be likened to the disparity between the Lagrange and Peano type remainder formulas in Taylor's theorem. Furthermore, two explanations are provided for the error formula with respect to the two parameters in the resolvent function. One explanation reveals that the MOR error is an interpolation remainder, while the other explanation implies that the error is also a Gauss-Christoffel quadrature remainder. By applying the error formula, we suggest a greedy algorithm for the interpolatory H_∞ norm MOR.

Key words. transfer function, rational Krylov subspace, Ritz value, H_∞ norm model order reduction

AMS subject classifications. 34C20, 41A05, 49K15, 49M05, 93A15, 93C05, 93C15

1. Introduction. We investigate the model error of model order reduction (MOR) [68], which involves rational Krylov subspace projection methods. The initial single-input-single-output (SISO) dynamical system is described as follows.

$$\begin{cases} \frac{dx(t)}{dt} = Ax(t) + bu(t), \\ y(t) = c^H x(t), \end{cases}$$

with $A \in \mathbb{C}^{n \times n}$ and $b, c \in \mathbb{C}^{n \times 1}$.

Using the rational Krylov subspaces $\text{span}(V)$ and $\text{span}(W)$, we obtain the reduced system:

$$\begin{cases} W^H V \frac{dx(t)}{dt} = W^H A V x(t) + W^H b u(t), \\ y(t) = c^H V x(t). \end{cases}$$

The transfer functions of these systems can be described as follows.

$$\begin{aligned} h(\mathfrak{s}) &= c^H (\mathfrak{s}I - A)^{-1} b, \\ \tilde{h}(\mathfrak{s}) &= c^H V (\mathfrak{s}W^H V - W^H A V)^{-1} W^H b. \end{aligned}$$

The model error can be measured by utilizing specific norms of $e(\mathfrak{s}) := h(\mathfrak{s}) - \tilde{h}(\mathfrak{s})$ [11, Section 7.2.3]. The well-known moments matching result states that $h^{(k)}(s_0) = \tilde{h}^{(k)}(s_0)$. This implies $e(\mathfrak{s}) = o((\mathfrak{s} - s_0)^k)$ near s_0 . This type of error can be likened to the Peano remainder in Taylor's theorem. When we do analysis on a wide region, this Peano type remainder is not satisfied. We are curious about the behavior of $e(\mathfrak{s})$ as \mathfrak{s} moves away from s_0 . In a word, this paper aims to address the following question: Considering that $\tilde{h}(\mathfrak{s})$ is the interpolating function of $h(\mathfrak{s})$, who can be identified as the interpolation remainder? The complexity of this problem stems from the fact that both $h(\mathfrak{s})$ and $\tilde{h}(\mathfrak{s})$ are rational functions and possess special forms. As a result, the existence of an explicit error formula was uncertain until the completion of this research.

The Krylov subspace projection method is one of the mainstream methods in the field of MOR. There are plenty of references related to this topic. We mainly review the literature which are closely related to

*Version of Dec 27, 2024.

[†]School of Economic and Mathematics, Southwestern University of Finance and Economics, Chengdu, China (yiding.lin@gmail.com). The work is supported by National Natural Science Foundation of China (NSFC-11526166, NSFC-12101508).

the (tangential) interpolation property and the moments matching theory. This type methods are first set up by Skelton *et al.* [20, 74, 75]. Then, Grimme combines it with the rational Krylov subspaces [38]. Gallivan, Vandendorpe and Van Dooren make several contributions to this topic [32–34]. A recent book [4] by Antoulas, Beattie and Gugercin summarizes the latest theories and algorithms. Other material can be found in [2, 5, 8, 12, 39, 49, 68] and references therein.

In 1997, Grimme [38] observed that the model error can be expressed as $e(\mathfrak{s}) = r_c^H(\mathfrak{s}I - A)^{-1}r_b$. This truth is used in later references (e.g. [6, 7, 26, 27, 62]). Our work starts by expanding r_b and r_c in relation to the Ritz values and the shifts. The expressions for the residual r via rational Krylov subspace methods are presented in [10, 22, 40, 45, 71]. The known expressions of the residual concern the Galerkin type (one-sided) projection process. When we generalize the residual expression for dealing with MOR, we replace it by the Petrov-Galerkin (two-sided) projection process, which is widely used in MOR [60, 62]. We explicitly express r_b and r_c through the utilization of special bases derived from the Lanczos biorthogonalization procedure. Thus, an explicit formula of $e(\mathfrak{s})$ is derived.

In the preceding research, we identify two further theoretical explanations for the model error. The explanations pertain to the two parameters in the resolvent function $\mathcal{H}(\lambda, \mathfrak{s}) = 1/(\mathfrak{s} - \lambda)$. With respect to the variable \mathfrak{s} , it can be observed that the error formula is, in fact, the interpolation remainder when the Hermitian formula is applied to the resolvent function.

The situation is more complicated with respect to the variable λ . It should be noted the Ritz values correspond to the quadrature nodes of Gauss-Christoffel quadrature. This motivates our research into the discovery of a correlation between the error formula and Gauss quadrature. The relevant theory for Hermitian A and $b = c$ is presented in book [50, Chapter 3] by Liesen and Strakoš. After a series of derivations, it can be concluded that the error formula is, in fact, a Gauss-Christoffel quadrature remainder.

Based on various error estimations, a multitude of adaptive algorithms for MOR have been developed [7, 27, 62]. In designing algorithms for the interpolatory H_∞ norm MOR, it is not appropriate to completely compute $e(s)$, since the explicit form of $e(s)$ contains the term $(\mathfrak{s}I - A)^{-1}$ inside. Following a thorough examination of the explicit error formula, we are able to derive certain approximations that can be computed in the reduced problems. Our two-sided greedy algorithms are then presented by modifying the one-sided projection algorithm in [22]. The next shifts are obtained by identifying the maximal point of the current error. Subsequently, the proposed algorithms are evaluated in comparison with other algorithms. The numerical experiments demonstrate a comparable behaviour of its error in the H_∞ norm to that of IRKA (which computes H_2 norm optimal MOR), while our algorithms require a considerably lesser CPU time.

The paper is structured as follows: In Section 2, we present the explicit error formula for the two-sided projection method, together with a proof and two further explanations. Section 3 provides the explicit error formula for the one-sided projection method. A similarity can be observed between the error in the l -order two-sided projection MOR and that of the $2l$ -order one-sided projection MOR. In Section 4, we present a review of the interpolatory H_∞ norm MOR and provide approximations of $e(\mathfrak{s})$ which can be computed in the reduced problems. Our greedy two-sided algorithms are presented in Section 5, and the numerical testing on benchmark problems is provided in Section 6. The conclusions are outlined in Section 7.

Notation: The standard Krylov subspace is represented by the following symbol:

$$\text{Krylov}(A, b, l) := \text{span}(b, Ab, \dots, A^{l-1}b). \quad (1.1)$$

The operation $\text{orth}(V)$ produces the orthonormal basis matrix of $\text{span}(V)$. The shifts sets for the left and right rational Krylov subspaces are, respectively, denoted by $\mathbb{T} = \{t_j\}_{j=1}^{k_c}$ and $\mathbb{S} = \{s_j\}_{j=1}^{k_b}$. Consequently, the rational Krylov subspaces can be written as follows:

$$\begin{aligned} \text{RK}(A, b, \mathbb{S}, k_b) &:= \text{span}\{(A - s_1 I)^{-1}b, (A - s_2 I)^{-1}(A - s_1 I)^{-1}b, \dots, \prod_{j=1}^{k_b} (A - s_j I)^{-1}b\}, \\ \text{RK}(A^H, c, \overline{\mathbb{T}}, k_c) &:= \text{span}\{(A - t_1 I)^{-H}c, (A - t_2 I)^{-H}(A - t_1 I)^{-H}c, \dots, \prod_{j=1}^{k_c} (A - t_j I)^{-H}c\}. \end{aligned} \quad (1.2)$$

The symbol $\mathbb{P}_m(\lambda)$ denotes the polynomial set, in which the degree of the polynomials is limited to m or less. In accordance with the polynomial $\varphi(\lambda)$, the symbol $\mathbb{P}_m(\lambda)/\varphi(\lambda)$ represent the rational function set. The numerator of its element is a polynomial of degree at most m . In addition, the symbol $\mathbb{Q}_{l-1,l}(\lambda)$ denotes the rational function set. The numerator of its element is of degree $l-1$, while the denominator is of degree l .

Write $\iota = \sqrt{-1}$. The set of A 's eigenvalues is denoted by $\text{eig}(A) = \{\lambda_i(A)\}_{i=1}^n$. The symbol $f[x_1, x_2, \dots, x_m]$ denotes the divided differences of the function $f(x)$. Unless otherwise specified, the norm $\|\cdot\|$ is an abbreviation of $\|\cdot\|_2$. The symbol Σ^- denotes the complement set of Σ . Matlab notations will be employed wherever feasible.

2. The error formula of the two-sided projection method. We commence with the definition of the combined Krylov (CK) subspaces.

$$\begin{aligned} \text{CK}(A, b, k_b, m_b) &:= \text{RK}(A, b, \mathbb{S}, k_b) + \text{Krylov}(A, b, m_b), \\ \text{CK}(A^H, c, k_c, m_c) &:= \text{RK}(A^H, c, \overline{\mathbb{T}}, k_c) + \text{Krylov}(A^H, c, m_c), \end{aligned} \quad (2.1)$$

where (rational) Krylov subspaces are defined by (1.1) and (1.2). With notations $l := k_b + m_b = k_c + m_c$ and

$$\varphi(\mathfrak{s}) := \prod_{j=1}^{k_b} (\mathfrak{s} - s_j), \quad \psi(\mathfrak{s}) := \prod_{j=1}^{k_c} (\mathfrak{s} - t_j), \quad (2.2)$$

we observe that (cf. Section 2.2.1)

$$\text{CK}(A, b, k_b, m_b) = \text{Krylov}(A, \varphi(A)^{-1}b, l), \quad \text{CK}(A^H, c, k_c, m_c) = \text{Krylov}(A^H, \psi(A)^{-H}c, l).$$

THEOREM 2.1. *Let V and W satisfy $\text{span}(V) = \text{CK}(A, b, k_b, m_b)$, $\text{span}(W) = \text{CK}(A^H, c, k_c, m_c)$ defined by (2.1). Suppose that the Lanczos biorthogonalization procedure of $[A, \varphi(A)^{-1}b, \psi(A)^{-H}c]$ does not break down until the $(l+1)$ th iteration. Let $\Lambda(\lambda) := \prod_{i=1}^l (\lambda - \lambda_i)$ be the monic characteristic polynomial of $(W^H V)^{-1} W^H A V$. With (2.2), write*

$$g_b(\lambda) := \frac{\Lambda(\lambda)}{\varphi(\lambda)}, \quad g_c(\lambda) := \frac{\Lambda(\lambda)}{\psi(\lambda)}. \quad (2.3)$$

Then, it holds that

$$\begin{aligned} e(\mathfrak{s}) &= h(\mathfrak{s}) - \tilde{h}(\mathfrak{s}) = c^H (\mathfrak{s}I - A)^{-1} b - c^H V (\mathfrak{s}W^H V - W^H A V)^{-1} W^H b \\ &= \frac{1}{g_b(\mathfrak{s})g_c(\mathfrak{s})} c^H g_c(A) (\mathfrak{s}I - A)^{-1} g_b(A) b. \end{aligned}$$

The proof is presented in three *steps*: Theorem 2.5, Theorem 2.9 and the final proof in Section 2.3. Furthermore, we possess Theorem 2.15 for the generalization onto the descriptor system. The proof is a constructive type one by using a Lanczos biorthogonalization procedure. The aforementioned assumption ensures $W^H V$ is nonsingular. We commence by presenting a series of observations.

1. The combined Krylov subspaces span the same subspaces as those described in [32, Definition 11]. The definition (2.1) employs the product-type bases, with no consideration on the multiplicity of the shifts. These special bases are a truncation of the one used in [48, Theorem 6.1]. They are one of the various bases of the rational Krylov subspace. The expressions of rational functions make it evident that they span the same subspace (cf. [40, Lemma 4.2(d)]).
2. It should be noted that $k_b + m_b = k_c + m_c$, but that k_b does not need to be equal to k_c . In order to encompass the greatest number of significant subspaces, our rational Krylov subspace was established as inclusively as possible. Theorem 2.1 presents a comprehensive result concerning the interpolation property. It directly gives rise to the moments matching results (e.g. [2, Proposition 11.7, Proposition 11.8, Proposition 11.10, Proposition 11.11]). From the explicit form of $e(\mathfrak{s})$, it is apparent that $e(\mathfrak{s})$ fully satisfies [32, Definition 16] (an equivalent condition of moments matching).

With (2.5), we easily observe that: For any complex \mathfrak{s} , it holds that

$$r_b \in \text{Krylov}(A, b, m+1) = \text{span}(V_{m+1}), \quad r_c \in \text{Krylov}(A^H, c, m+1) = \text{span}(W_{m+1}).$$

We define the polynomial expressions:

$$\begin{aligned} x_b &= \chi_b(A, \mathfrak{s})b, & \chi_b(\lambda, \mathfrak{s}) &\in \mathbb{P}_{m-1}(\lambda), \\ r_b &= \gamma_b(A, \mathfrak{s})b, & \gamma_b(\lambda, \mathfrak{s}) &\in \mathbb{P}_m(\lambda). \end{aligned}$$

Their relations are given by

$$\begin{aligned} r_b &= b - (\mathfrak{s}I - A)x_b, \\ \gamma_b(\lambda, \mathfrak{s}) &= 1 - (\mathfrak{s} - \lambda)\chi_b(\lambda, \mathfrak{s}), \\ \chi_b(\lambda, \mathfrak{s}) &= \frac{1 - \gamma_b(\lambda, \mathfrak{s})}{\mathfrak{s} - \lambda}. \end{aligned}$$

We easily find $\gamma_b(\lambda, \mathfrak{s})$ satisfies a constraint condition:

$$\gamma_b(\mathfrak{s}, \mathfrak{s}) = 1. \quad (2.6)$$

Similar to [61, (3.8)] and [36, Theorem 3.1], we deduce the polynomial formulas for the residuals.

LEMMA 2.4. *Suppose relations (2.4) hold. Then, it holds that*

$$\begin{aligned} r_b &= \gamma_b(A, \mathfrak{s})b, & r_c^H &= c^H \gamma_c(A, \mathfrak{s}), \\ \gamma_b(\lambda, \mathfrak{s}) &= \gamma_c(\lambda, \mathfrak{s}) = \frac{\Lambda(\lambda)}{\Lambda(\mathfrak{s})}, \end{aligned}$$

where $\Lambda(\lambda) := \prod_{i=1}^m (\lambda - \lambda_i)$ is the monic characteristic polynomial of $T_m = W^H AV$.

Proof. We observe that $r_b \in \text{Krylov}(A, b, m+1)$ and $r_b \perp \text{Krylov}(A^H, c, m)$. By Lemma 2.3, we directly obtain $r_b = \rho \Lambda(A)b$, where $\Lambda(\lambda)$ is the monic characteristic polynomial of $T_m = W^H AV$. Obviously, when \mathfrak{s} varies, ρ changes. Thus, we can regard ρ as a function of the variable \mathfrak{s} . It implies that $\gamma_b(\lambda, \mathfrak{s}) = \rho(\mathfrak{s})\Lambda(\lambda)$. By the constraint condition (2.6), we directly obtain $\rho(\mathfrak{s}) = 1/\Lambda(\mathfrak{s})$ and then $\gamma_b(\lambda, \mathfrak{s}) = \Lambda(\lambda)/\Lambda(\mathfrak{s})$. Similarly, we get the result about r_c . \square

THEOREM 2.5. *Suppose the Lanczos biorthogonalization procedure of (A, b, c) does not break down until the $(m+1)$ th iteration. The relations of the formed matrices are given by (2.4). Then, it holds that*

$$\begin{aligned} h(\mathfrak{s}) - \tilde{h}(\mathfrak{s}) &= c^H (\mathfrak{s}I - A)^{-1} b - c^H V (\mathfrak{s}W^H V - W^H AV)^{-1} W^H b \\ &= c^H (\mathfrak{s}I - A)^{-1} b - c^H V (\mathfrak{s}I - W^H AV)^{-1} W^H b \\ &= \frac{1}{[\Lambda(\mathfrak{s})]^2} c^H (\mathfrak{s}I - A)^{-1} [\Lambda(A)]^2 b, \end{aligned}$$

where $\Lambda(\lambda) := \prod_{i=1}^m (\lambda - \lambda_i)$ is the monic characteristic polynomial of $T_m = W^H AV$.

Proof. Note that

$$\begin{aligned} r_b &= b - (\mathfrak{s}I - A)x_b, \\ (\mathfrak{s}I - A)^{-1} b - x_b &= (\mathfrak{s}I - A)^{-1} r_b, \\ c^H (\mathfrak{s}I - A)^{-1} b - c^H x_b &= c^H (\mathfrak{s}I - A)^{-1} r_b, \\ \text{similarly, } c^H (\mathfrak{s}I - A)^{-1} &= r_c^H (\mathfrak{s}I - A)^{-1} + x_c^H. \end{aligned}$$

Since $x_c \in \text{Krylov}(A^H, c, m)$ and $r_b \perp \text{Krylov}(A^H, c, m)$, we know $x_c^H r_b = 0$. By Lemma 2.4, we obtain

$$\begin{aligned} e(\mathfrak{s}) &= h(\mathfrak{s}) - \tilde{h}(\mathfrak{s}) = c^H(\mathfrak{s}I - A)^{-1}b - c^H x_b = c^H(\mathfrak{s}I - A)^{-1}r_b = [r_c^H(\mathfrak{s}I - A)^{-1} + x_c^H]r_b \\ &= r_c^H(\mathfrak{s}I - A)^{-1}r_b = c^H \frac{\Lambda(A)}{\Lambda(\mathfrak{s})}(\mathfrak{s}I - A)^{-1} \frac{\Lambda(A)}{\Lambda(\mathfrak{s})}b = \frac{1}{[\Lambda(\mathfrak{s})]^2} c^H(\mathfrak{s}I - A)^{-1}[\Lambda(A)]^2 b. \end{aligned}$$

□

REMARK 2.6. The relation (2.4) requires $c^H b = 1$, which is not a common occurrence in practice. Nevertheless, this has no impact on the result of Theorem 2.5. The coefficient $m_0 := c^H b$ is indeed the first moment of $c^H A^i b$ [63, (2.1)]. Note that $h(\mathfrak{s}) = c^H(\mathfrak{s}I - A)^{-1}b = m_0 c^H(\mathfrak{s}I - A)^{-1}(b/m_0)$. If $m_0 \neq 1$, then the conclusions of Theorem 2.5 remain valid, after our applying Theorem 2.5 onto $(A, b/m_0, c)$ and multiplying the resulting expression by m_0 .

The relation $e(\mathfrak{s}) = r_c^H(\mathfrak{s}I - A)^{-1}r_b$ is known in Grimme's PhD thesis [38, Theorem 5.1]. The traditional result shows that $e(\mathfrak{s}) = O(1/\mathfrak{s}^{2m+1})$ (e.g. [2, Section 11.2.1] [50, (3.3.26)]). We now present a clear and explicit formulation of the error.

2.2. Step 2: General subspaces (rational Krylov subspaces) and special bases.

2.2.1. Biorthogonal bases of $\text{CK}(A, b, k_b, m_b)$ and $\text{CK}(A^H, c, k_c, m_c)$. The rational Krylov subspace can be obtained by a special standard Krylov subspace (e.g. [40, Lemma 4.2(a)]). With (2.1), we have

$$\begin{aligned} \text{CK}(A, b, k_b, m_b) &= \text{Krylov}(A, \varphi(A)^{-1}b, l), & \text{CK}(A, b, k_b, m_b + 1) &= \text{Krylov}(A, \varphi(A)^{-1}b, l + 1), \\ \text{CK}(A^H, c, k_c, m_c) &= \text{Krylov}(A^H, \psi(A)^{-H}c, l), & \text{CK}(A^H, c, k_c, m_c + 1) &= \text{Krylov}(A^H, \psi(A)^{-H}c, l + 1). \end{aligned} \quad (2.7)$$

We use the Lanczos biorthogonalization procedure of A , $\varphi(A)^{-1}b$ and $\psi(A)^{-H}c$ to form the biorthogonal bases of $\text{Krylov}(A, \varphi(A)^{-1}b, l + 1)$ and $\text{Krylov}(A^H, \psi(A)^{-H}c, l + 1)$. The relations are summarized as follows.

$$\begin{aligned} \hat{v}_1 &= \varphi(A)^{-1}b, & \hat{w}_1 &= \psi(A)^{-H}c, & \hat{w}_1^H \hat{v}_1 &= 1, \\ A\hat{V}_l &= \hat{V}_{l+1}\hat{T}_l, & \text{span}(\hat{V}_l) &= \text{Krylov}(A, \varphi(A)^{-1}b, l), & \text{span}(\hat{V}_{l+1}) &= \text{Krylov}(A, \varphi(A)^{-1}b, l + 1), \\ A^H\hat{W}_l &= \hat{W}_{l+1}\hat{K}_l, & \text{span}(\hat{W}_l) &= \text{Krylov}(A^H, \psi(A)^{-H}c, l), & \text{span}(\hat{W}_{l+1}) &= \text{Krylov}(A^H, \psi(A)^{-H}c, l + 1), \\ \hat{W}_l^H \hat{V}_l &= I, & \hat{W}_{l+1}^H \hat{V}_{l+1} &= I, & \hat{W}_l^H A\hat{V}_l &= \hat{T}_l, & \hat{V}_l^H A^H \hat{W}_l &= \hat{K}_l, & \hat{T}_l &= \hat{K}_l^H, \end{aligned} \quad (2.8)$$

$$\hat{T}_{l+1} = \begin{bmatrix} \hat{\alpha}_1 & \hat{\beta}_2 & & & & \\ \hat{\gamma}_2 & \hat{\alpha}_2 & \hat{\beta}_3 & & & \\ & \ddots & \ddots & \ddots & & \\ & & & \hat{\gamma}_{l-1} & \hat{\alpha}_{l-1} & \hat{\beta}_l \\ & & & & \hat{\gamma}_l & \hat{\alpha}_l \\ \hline & & & & & \hat{\gamma}_{l+1} \end{bmatrix} = \begin{bmatrix} \hat{T}_m \\ \hat{\gamma}_{m+1} e_m^H \end{bmatrix}.$$

As in Section 2.1.2, we adopt the same notations for x_b, x_c, r_b, r_c and their rational function expressions. The two-sided projection (Petrov-Galerkin) conditions are imposed as follows:

$$\begin{aligned} x_b &\in \text{CK}(A, b, k_b, m_b), & r_b &= b - (\mathfrak{s}I - A)x_b \in \text{CK}(A, b, k_b, m_b + 1), \\ \text{s.t. } r_b &\perp \text{CK}(A^H, c, k_c, m_c), \end{aligned} \quad (2.9)$$

and

$$\begin{aligned} x_c &\in \text{CK}(A^H, c, k_c, m_c), & r_c &= c - (\mathfrak{s}I - A)^H x_c \in \text{CK}(A^H, c, k_c, m_c + 1), \\ \text{s.t. } r_c &\perp \text{CK}(A, b, k_b, m_b). \end{aligned}$$

Thus, we get $\tilde{h}(\mathfrak{s}) = x_c^H b = c^H x_b$, where

$$x_b = \widehat{V}(\mathfrak{s}I - \widehat{W}^H A \widehat{V})^{-1} \widehat{W}^H b, \quad x_c = \widehat{W}(\mathfrak{s}I - \widehat{W}^H A \widehat{V})^{-H} \widehat{V}^H c.$$

By (2.7), the rational function expressions are as follows:

$$\begin{aligned} x_b &= \chi_b(A, \mathfrak{s})b, & \chi_b(\lambda, \mathfrak{s}) &\in \mathbb{P}_{l-1}(\lambda)/\varphi(\lambda), \\ r_b &= \gamma_b(A, \mathfrak{s})b, & \gamma_b(\lambda, \mathfrak{s}) &\in \mathbb{P}_l(\lambda)/\varphi(\lambda). \end{aligned}$$

Their relations are given by the following formulas.

$$\begin{aligned} r_b &= b - (\mathfrak{s}I - A)x_b, \\ \gamma_b(\lambda, \mathfrak{s}) &= 1 - (\mathfrak{s} - \lambda)\chi_b(\lambda, \mathfrak{s}), \\ \chi_b(\lambda, \mathfrak{s}) &= \frac{1 - \gamma_b(\lambda, \mathfrak{s})}{\mathfrak{s} - \lambda}. \end{aligned} \tag{2.10}$$

Therefore, we still have the constraint condition: $\gamma_b(\mathfrak{s}, \mathfrak{s}) = 1$.

2.2.2. The derivation. Prior to the presentation of the final expressions of r_b and r_c derived from the two-sided projection method, it is noteworthy to mention that the residual expression from the one-sided projection method has been derived by other approaches (e.g. [45, (3.5)] [40, (7.17)]). The result has been employed for the purposes of theoretical analysis [10] and algorithms development [22, 71].

LEMMA 2.7. *Suppose relations (2.8) hold. Set $g_b(\mathfrak{s}) := \Lambda(\mathfrak{s})/\varphi(\mathfrak{s})$ and $g_c(\mathfrak{s}) := \Lambda(\mathfrak{s})/\psi(\mathfrak{s})$, where $\Lambda(\lambda)$ is the monic characteristic polynomial of $\widehat{T}_l = \widehat{W}^H A \widehat{V}$. Then, it holds that*

$$\begin{aligned} \gamma_b(\lambda, \mathfrak{s}) &= \frac{g_b(\lambda)}{g_b(\mathfrak{s})}, & r_b &= \gamma_b(A, \mathfrak{s})b, \\ \gamma_c(\lambda, \mathfrak{s}) &= \frac{g_c(\lambda)}{g_c(\mathfrak{s})}, & r_c^H &= c^H \gamma_c(A, \mathfrak{s}). \end{aligned}$$

Proof. After translating (2.9) into the standard Krylov subspace language with (2.7), we obtain

$$\begin{aligned} x_b &\in \text{Krylov}(A, b, l), & r_b &= b - (\mathfrak{s}I - A)x_b \in \text{Krylov}(A, \varphi(A)^{-1}b, l + 1), \\ \text{s.t. } r_b &\perp \text{Krylov}(A^H, \psi(A)^{-H}c, l). \end{aligned}$$

By Lemma 2.3, we directly obtain $r_b = \rho \Lambda(A)[\varphi(A)^{-1}b] = \rho g_b(A)b$, where $\Lambda(\lambda)$ is the monic characteristic polynomial of \widehat{T}_l . As \mathfrak{s} varies, so does the coefficient ρ . Thus, we can regard ρ as a function of the variable \mathfrak{s} . With a new symbol $\rho(\mathfrak{s})$, we obtain

$$\gamma_b(\lambda, \mathfrak{s}) = \rho(\mathfrak{s}) \frac{\Lambda(\lambda)}{\varphi(\lambda)} = \rho(\mathfrak{s}) g_b(\lambda).$$

Given the constraint condition $\gamma_b(\mathfrak{s}, \mathfrak{s}) = 1$, it follows that $\rho(\mathfrak{s}) = 1/g_b(\mathfrak{s})$. Hence, $\gamma_b(\lambda, \mathfrak{s}) = g_b(\lambda)/g_b(\mathfrak{s})$. Similarly, we shall obtain the result about r_c . \square

REMARK 2.8. *By relation (2.10), we obtain a new expression of $\tilde{h}(\mathfrak{s}) = c^H x_b = x_c^H b$:*

$$\begin{aligned} \tilde{h}(\mathfrak{s}) &= c^H \chi_b(A, \mathfrak{s})b = c^H \chi_c(A, \mathfrak{s})b, \\ \chi_b(\lambda, \mathfrak{s}) &= \frac{1 - \gamma_b(\lambda, \mathfrak{s})}{\mathfrak{s} - \lambda}, & \chi_c(\lambda, \mathfrak{s}) &= \frac{1 - \gamma_c(\lambda, \mathfrak{s})}{\mathfrak{s} - \lambda}. \end{aligned}$$

THEOREM 2.9. *Suppose the Lanczos biorthogonalization procedure of $[A, \varphi(A)^{-1}b, \psi(A)^{-H}c]$ does not break down until $(l+1)$ th iteration. The formed matrices satisfy (2.8). Then, it holds that*

$$\begin{aligned} h(\mathfrak{s}) - \tilde{h}(\mathfrak{s}) &= c^H(\mathfrak{s}I - A)^{-1}b - c^H\widehat{V}(\mathfrak{s}I - \widehat{W}^H A \widehat{V})^{-1}\widehat{W}^H b \\ &= r_c^H(\mathfrak{s}I - A)^{-1}r_b \\ &= \frac{1}{g_b(\mathfrak{s})g_c(\mathfrak{s})}c^H g_c(A)(\mathfrak{s}I - A)^{-1}g_b(A)b, \end{aligned}$$

where $\Lambda(\lambda)$ is the monic characteristic polynomial of $\widehat{T}_l = \widehat{W}^H A \widehat{V}$.

The proof is straightforward. By substituting the result of Lemma 2.7 into $e(\mathfrak{s}) = r_c^H(\mathfrak{s}I - A)^{-1}r_b$, we obtain the desired result. The assumption $c^H\psi(A)^{-1}\varphi(A)^{-1}b = 1$ in (2.8) also does not affect the result. The discussion is analogous to an earlier discussion of $c^H b = 1$ for Theorem 2.5, as stated in Remark 2.6. In essence, we obtain the explicit error formula by utilizing special bases \widehat{V} and \widehat{W} of general subspaces $\text{CK}(A, b, k_b, m_b)$ and $\text{CK}(A^H, c, k_c, m_c)$.

2.3. Step 3: General subspaces and general bases. We give the final proof of Theorem 2.1.

Proof. Let \widehat{V} and \widehat{W} be the special bases used in Theorem 2.5. They satisfy $\text{span}(\widehat{V}_l) = \text{CK}(A, b, k_b, m_b)$, $\text{span}(\widehat{W}_l) = \text{CK}(A^H, c, k_c, m_c)$ and $\widehat{W}^H \widehat{V} = I$.

Because of $\text{span}(V) = \text{CK}(A, b, k_b, m_b)$ and $\text{span}(W) = \text{CK}(A^H, c, k_c, m_c)$, we obtain the relations $V = \widehat{V}R$ and $W = \widehat{W}S$, where both R and S are nonsingular transformation matrices. Then, it holds that

$$\begin{aligned} \tilde{h}(\mathfrak{s}) &= c^H V(\mathfrak{s}W^H V - W^H A V)^{-1}W^H b = c^H \widehat{V}R(zS^H \widehat{W}^H \widehat{V}R - S^H \widehat{W}^H A \widehat{V}R)^{-1}S^H \widehat{W}^H b \\ &= c^H \widehat{V}(z\widehat{W}^H \widehat{V} - \widehat{W}^H A \widehat{V})^{-1}\widehat{W}^H b = c^H \widehat{V}(zI - \widehat{W}^H A \widehat{V})^{-1}\widehat{W}^H b. \end{aligned}$$

By Theorem 2.9, we obtain

$$h(\mathfrak{s}) - \tilde{h}(\mathfrak{s}) = \frac{1}{g_b(\mathfrak{s})g_c(\mathfrak{s})}c^H g_c(A)(\mathfrak{s}I - A)^{-1}g_b(A)b,$$

where $\lambda_i (i = 1, 2, \dots, l)$ are eigenvalues of $\widehat{W}^H A \widehat{V}$. In this formula, the only elements related to the bases \widehat{V} and \widehat{W} are the eigenvalues. Let us now see how to relate these eigenvalues to the bases V and W . Obviously, we have $\text{eig}(\widehat{W}^H A \widehat{V}) = \text{eig}(S^{-H}W^H A V R^{-1}) = \text{eig}((S^H R)^{-1}W^H A V) = \text{eig}((W^H V)^{-1}W^H A V)$. \square

Researchers have already utilized the rational biorthogonal bases to design MOR [6, 7, 26, 27]. For a theoretical analysis of rational biorthogonal bases, see [73]. Since the error formula is independent of the bases, it is recommended that both V and W be orthonormal in practical implementation. They satisfy $V_l^H V_l = I$, $W_l^H W_l = I$ and $W_l^H V_l \neq I$, where $\text{span}(V_l) = \text{CK}(A, b, k_b, m_b)$ and $\text{span}(W_l) = \text{CK}(A^H, c, k_c, m_c)$. To obtain the orthonormal bases, we can apply Arnoldi-like procedure onto bases (2.1). If the shifts sets \mathbb{T} and \mathbb{S} are given, a more convenient approach is to call *A Rational Krylov Toolbox for MATLAB* [16].

With the new notation

$$G_{\text{two}}(\lambda) := g_b(\lambda)g_c(\lambda) = \frac{\Lambda(\lambda)}{\varphi(\lambda)} \frac{\Lambda(\lambda)}{\psi(\lambda)}, \quad (2.11)$$

the error formula is simplified as follows.

$$e(\mathfrak{s}) = h(\mathfrak{s}) - \tilde{h}(\mathfrak{s}) = \frac{1}{G_{\text{two}}(\mathfrak{s})}c^H(\mathfrak{s}I - A)^{-1}G_{\text{two}}(A)b. \quad (2.12)$$

2.4. Two further explanations for the MOR error. The explicit identification of the error formula allows for the deeper comprehension of the fundamental characteristics of the MOR error. We discover two further explanations for the MOR error, which are closely related to the two parameters of the resolvent function

$\mathcal{H}(\lambda, \mathfrak{s}) = 1/(\mathfrak{s} - \lambda)$. The MOR error can be classified as either an interpolation remainder with respect to variable \mathfrak{s} or a quadrature remainder with respect to λ . In order to provide a concise presentation, the demonstration will primarily focus on how the terms within MOR correspond to those within the classical interpolation (or quadrature) theory. The omitted proofs can be located in the preceding version of the manuscript [51].

In interpolation theory, the Lagrange-type remainder can be applied if all of the nodes are real (e.g. [1, Theorem 1]). Given that all of the shifts and Ritz values in our problem are complex, it is vital to utilize alternative theoretical tools. Our theoretical tool is the Hermitian remainder or the divided difference remainder. The Hermitian formula represents the Cauchy integral form of the interpolation remainder (e.g. [47, (8)] [31, Page 59]). After transforming the polynomial function to the rational function [40, Page 33], we can derive an error formula for rational function interpolation, which is named as the Walsh-Hermite formula in [41, Page 19].

LEMMA 2.10. (Hermite) *Suppose the boundary Γ of Σ consists of finitely many rectifiable Jordan curves with positive orientation relative to Σ , and suppose $M(\mathfrak{s})$ is analytic in Σ and continuous in $\Sigma \cup \Gamma$. Suppose the interpolation conditions hold, i.e., $M(\alpha_i) = P_{k-1}(\alpha_i)$ for $\alpha_i \in \Sigma (i = 1, 2, \dots, k)$. Write $\pi_k^\alpha(\mathfrak{s}) = \prod_{i=1}^k (\mathfrak{s} - \alpha_i)$. Then, it holds that*

$$M(\mathfrak{s}) - P_{k-1}(\mathfrak{s}) = \frac{1}{2\pi i} \oint_{\Gamma} \frac{\pi_k^\alpha(\mathfrak{s})}{\pi_k^\alpha(\zeta)} \frac{M(\zeta)}{\zeta - \mathfrak{s}} d\zeta.$$

LEMMA 2.11. (Walsh-Hermite) *Let $Q_{k-1,k}(\mathfrak{s}) \in \mathbb{Q}_{k-1,k}(\mathfrak{s})$ be a rational interpolating function of $N(\mathfrak{s})$ with poles β_i and interpolation nodes α_i . Write*

$$G_k^{\alpha,\beta}(\mathfrak{s}) := \prod_{i=1}^k \frac{z - \alpha_i}{z - \beta_i} = \frac{(\mathfrak{s} - \alpha_1)(\mathfrak{s} - \alpha_2) \cdots (\mathfrak{s} - \alpha_k)}{(\mathfrak{s} - \beta_1)(\mathfrak{s} - \beta_2) \cdots (\mathfrak{s} - \beta_k)}.$$

Suppose the boundary Γ of Σ consists of finitely many rectifiable Jordan curves with positive orientation relative to Σ , and suppose $N(\mathfrak{s})$ is analytic in Σ and continuous in $\Sigma \cup \Gamma$. If interpolation nodes $\alpha_i (i = 1, 2, \dots, k)$ are in Σ , then it holds that

$$N(\mathfrak{s}) - Q_{k-1,k}(\mathfrak{s}) = \frac{1}{2\pi i} \oint_{\Gamma} \frac{G_k^{\alpha,\beta}(\mathfrak{s})}{G_k^{\alpha,\beta}(\zeta)} \frac{N(\zeta)}{\zeta - \mathfrak{s}} d\zeta.$$

Proof. Let $\pi_k^\beta(\mathfrak{s}) := \prod_{i=1}^k (\mathfrak{s} - \beta_i)$, $\tilde{N}(\mathfrak{s}) := N(\mathfrak{s})\pi_k^\beta(\mathfrak{s})$ and $P_{k-1}(\mathfrak{s}) := Q_{k-1,k}(\mathfrak{s})\pi_k^\beta(\mathfrak{s})$. By the rational interpolation condition, we obtain $\tilde{N}(\alpha_i) = P_{k-1}(\alpha_i)$ for $\alpha_i \in \Sigma (i = 1, 2, \dots, k)$. Thus, Lemma 2.10 is applied.

$$N(\mathfrak{s})\pi_k^\beta(\mathfrak{s}) - P_{k-1}(\mathfrak{s}) = \tilde{N}(\mathfrak{s}) - P_{k-1}(\mathfrak{s}) = \frac{1}{2\pi i} \oint_{\Gamma} \frac{\pi_k^\alpha(\mathfrak{s})}{\pi_k^\alpha(\zeta)} \frac{\tilde{N}(\zeta)}{\zeta - \mathfrak{s}} d\zeta = \frac{1}{2\pi i} \oint_{\Gamma} \frac{\pi_k^\alpha(\mathfrak{s})}{\pi_k^\alpha(\zeta)} \frac{N(\zeta)\pi_k^\beta(\zeta)}{\zeta - \mathfrak{s}} d\zeta. \quad (2.13)$$

The proof is completed after our dividing (2.13) by $\pi_k^\beta(\mathfrak{s})$. \square

In the next two subsections, we apply Lemma 2.11 onto the resolvent function $\mathcal{H}(\lambda, \mathfrak{s}) = 1/(\mathfrak{s} - \lambda)$ with respect to variables \mathfrak{s} and λ , respectively. Note that the interpolation nodes and poles of these two cases are opposite. The key step in the following proofs is the interchange between the problem resolvent function $\mathcal{H}(\lambda, \mathfrak{s})$ and the resolvent function in the Cauchy integral. Therefore, if other problems (e.g. [41, Section 4.2, Section 4.3]) lack a resolvent function term inside, we may not expect to acquire an explicit error formula.

2.4.1. Variable \mathfrak{s} . To make use of Lemma 2.11, we substitute $h(\mathfrak{s}) \in \mathbb{Q}_{n-1,n}(\mathfrak{s})$ and $\tilde{h}(\mathfrak{s}) \in \mathbb{Q}_{l-1,l}(\mathfrak{s})$ into $N(\mathfrak{s})$ and $Q_{k-1,k}(\mathfrak{s})$, respectively. For simplicity, we assume that $k_b = k_c = l$ and that all of the shifts t_i, s_i (from $\varphi(\lambda), \psi(\lambda)$) are finite. Consider a region Σ such that $\text{eig}(A) \cup \{\lambda_i\} \subseteq \Sigma$ and $\{s_i, t_i\} \subseteq \Sigma^-$. We observe that $\tilde{h}(\mathfrak{s})$ is a rational interpolating function of $h(\mathfrak{s})$ with poles λ_i (doubled) and interpolation nodes t_i, s_i . Thus, we substitute $G_k^{\alpha,\beta}(\mathfrak{s}) = 1/G_{\text{two}}(\mathfrak{s})$ into Lemma 2.11, where $G_{\text{two}}(\mathfrak{s})$ is defined by (2.11). It is easy to check that

$h(\mathfrak{s})$ is analytic on Σ^- . By Lemma 2.11, for $\mathfrak{s} \in \Sigma^-$, it holds that

$$\begin{aligned} h(\mathfrak{s}) - \tilde{h}(\mathfrak{s}) &= \frac{1}{2\pi\iota} \oint_{\Gamma^-} \frac{G_k^{\alpha,\beta}(\mathfrak{s})}{G_k^{\alpha,\beta}(\zeta)} \frac{h(\zeta)}{\zeta - \mathfrak{s}} d\zeta = \frac{1}{2\pi\iota} \oint_{\Gamma^-} \frac{G_{\text{two}}(\zeta)}{G_{\text{two}}(\mathfrak{s})} \frac{c^H(\zeta I - A)^{-1}b}{\zeta - \mathfrak{s}} d\zeta \\ &= \frac{1}{G_{\text{two}}(\mathfrak{s})} \frac{1}{2\pi\iota} c^H \left[\oint_{\Gamma^-} \frac{G_{\text{two}}(\zeta)}{\zeta - \mathfrak{s}} (\zeta I - A)^{-1} d\zeta \right] b \\ &= \frac{1}{G_{\text{two}}(\mathfrak{s})} \frac{1}{2\pi\iota} c^H \left[\oint_{\Gamma} \frac{G_{\text{two}}(\zeta)}{\mathfrak{s} - \zeta} (\zeta I - A)^{-1} d\zeta \right] b \\ &= \frac{1}{G_{\text{two}}(\mathfrak{s})} c^H G_{\text{two}}(A) (\mathfrak{s} I - A)^{-1} b. \end{aligned}$$

In the last equality, we utilize the Cauchy integral definition for functions of matrices (e.g. [42, Definition 1.11]), given that $G_{\text{two}}(\zeta)/(\mathfrak{s} - \zeta)$ with respect to ζ is analytic on $\Sigma \supseteq \text{eig}(A) \cup \{\lambda_i\}$.

The following serves to provide an outline of the explanation with respect to variable \mathfrak{s} . In essence, it can be regarded as an interpolation formula. The functions $h(\mathfrak{s})$ and $\tilde{h}(\mathfrak{s})$ represent the interpolated and the interpolating functions, respectively. The moments matching theory states that the interpolation nodes are the shifts t_i, s_i [32]. Following the discovery that the order of the poles, λ_i , is two, it becomes evident that the MOR error $e(\mathfrak{s})$ can be regarded as the remainder of the interpolation formula.

2.4.2. Variable λ . With respect to the parameter λ , the initial step will be to construct the classical Hermitian interpolating polynomial, incorporating either the Hermitian remainder or the divided difference remainder. Subsequently, the Gauss quadrature is employed. We shall substitute $\widehat{\mathcal{H}}(\lambda) = \varphi(\lambda)\psi(\lambda)/(\mathfrak{s} - \lambda)$ into $\tilde{N}(\mathfrak{s})$ in (2.13). Now, the variable of interest is λ . For simplicity, we assume that there exists a set Σ satisfying $\text{eig}(A) \cup \{\lambda_i\} \subseteq \Sigma$ and $\{s_i, t_i\} \subseteq \Sigma^-$. In order to provide a concise explanation, it is assumed that all of $\{\lambda_i\}$ are distinct. Otherwise, the Gauss quadrature process is known to become more complicated [63, (4.1)].

PROPOSITION 2.12. *Let $\tilde{\mathcal{P}}_{2l-1}(\lambda) \in \mathbb{P}_{2l-1}(\lambda)$ be the Hermitian interpolating polynomial of $\widehat{\mathcal{H}}(\lambda)$ on the interpolation nodes λ_i (doubled). Then, the interpolation remainder can be expressed as follows:*

$$\begin{aligned} \widehat{\mathcal{H}}(\lambda) - \tilde{\mathcal{P}}_{2l-1}(\lambda) &= [\Lambda(\lambda)]^2 \widehat{\mathcal{H}}[\lambda_1, \lambda_1, \lambda_2, \lambda_2, \dots, \lambda_l, \lambda_l, \lambda], \\ \widehat{\mathcal{H}}[\lambda_1, \lambda_1, \lambda_2, \lambda_2, \dots, \lambda_l, \lambda_l, \lambda] &= \left\{ \frac{\varphi(\mathfrak{s})\psi(\mathfrak{s})}{[\Lambda(\mathfrak{s})]^2} \right\} \frac{1}{\mathfrak{s} - \lambda}. \end{aligned} \quad (2.14)$$

Proof. One of the explicit expressions of $\tilde{\mathcal{P}}_{2l-1}(\lambda)$ is given as follows (e.g. [17, Theorem 3.9]).

$$\begin{aligned} \widehat{\mathcal{H}}(\lambda_i) &= \tilde{\mathcal{P}}_{2l-1}(\lambda_i), \quad \widehat{\mathcal{H}}'(\lambda_i) = \tilde{\mathcal{P}}'_{2l-1}(\lambda_i), \quad i = 1, 2, \dots, l, \\ \tilde{\mathcal{P}}_{2l-1}(\lambda) &= \sum_{i=1}^l \widehat{\mathcal{H}}(\lambda_i) \{ \widehat{\mathcal{L}}_i^2(\lambda) [1 - 2(\lambda - \lambda_i)] \widehat{\mathcal{L}}_i'(\lambda) \} + \sum_{i=1}^l \widehat{\mathcal{H}}'(\lambda_i) [(\lambda - \lambda_i) \widehat{\mathcal{L}}_i^2(\lambda)], \end{aligned}$$

where $\widehat{\mathcal{L}}_i(\lambda)$ is the Lagrange basis polynomial

$$\widehat{\mathcal{L}}_i(\lambda) = \prod_{j=1, j \neq i}^l \frac{\lambda - \lambda_j}{\lambda_i - \lambda_j}.$$

This remainder formula is, in fact, a quantity equality, which permits a relatively straightforward proof. A proof based on the meanings of the divided difference can be found in [51, Lemma 2.15 and (2.24)].

An additional proof is provided by using Lemma 2.10. In this proof, an observation is made regarding the

interchange between the problem resolvent function $\mathcal{H}(\lambda, \mathfrak{s})$ and the resolvent function in the Cauchy integral.

$$\begin{aligned}
\widehat{\mathcal{H}}(\lambda) - \widetilde{\mathcal{P}}_{2l-1}(\lambda) &= \frac{1}{2\pi l} \oint_{\Gamma} \frac{[\Lambda(\lambda)]^2 \widehat{\mathcal{H}}(\zeta)}{[\Lambda(\zeta)]^2 \zeta - \lambda} d\zeta = [\Lambda(\lambda)]^2 \frac{1}{2\pi l} \oint_{\Gamma} \frac{1}{[\Lambda(\zeta)]^2} \frac{\varphi(\zeta)\psi(\zeta)}{\mathfrak{s} - \zeta} \frac{1}{\zeta - \lambda} d\zeta \\
&= [\Lambda(\lambda)]^2 \frac{1}{2\pi l} \oint_{\Gamma} \frac{1}{[\Lambda(\zeta)]^2} \frac{\varphi(\zeta)\psi(\zeta)}{\lambda - \zeta} \frac{1}{\zeta - \mathfrak{s}} d\zeta = [\Lambda(\lambda)]^2 \frac{1}{2\pi l} \oint_{\Gamma^-} \left\{ \frac{1}{[\Lambda(\zeta)]^2} \frac{\varphi(\zeta)\psi(\zeta)}{\zeta - \lambda} \right\} \frac{1}{\zeta - \mathfrak{s}} d\zeta \\
&= [\Lambda(\lambda)]^2 \frac{1}{[\Lambda(\mathfrak{s})]^2} \frac{\varphi(\mathfrak{s})\psi(\mathfrak{s})}{\mathfrak{s} - \lambda} = [\Lambda(\lambda)]^2 \widehat{\mathcal{H}}[\lambda_1, \lambda_1, \lambda_2, \lambda_2, \dots, \lambda_l, \lambda_l, \lambda].
\end{aligned} \tag{2.15}$$

The Cauchy integral formula is employed in the penultimate equality, given that the function in the braces with respect to ζ is analytic on Σ^- . \square

Once the interpolation phase is complete, the Gauss quadrature stage begins, which is now expressed as a linear functional. We begin by presenting two propositions pertaining to the classical result in Gauss quadrature.

PROPOSITION 2.13. *Suppose (2.8) hold. Then, it holds that $c^H \psi(A)^{-1} \mathcal{P}(A) \varphi(A)^{-1} b = e_1^H \mathcal{P}(\widehat{T}_l) e_1$ for any $\mathcal{P}(\lambda) \in \mathbb{P}_{2l-1}$.*

Proof. By (2.8), the relating matrices are formed by the Lanczos biorthogonalization procedure of A , $\varphi(A)^{-1} b$ and $\psi(A)^{-H} c$. Accordingly, the proof is completed by means of a direct application of the classical result ([29, Theorem 2]) onto A , $\varphi(A)^{-1} b$ and $\psi(A)^{-H} c$. \square

PROPOSITION 2.14. *Suppose relations (2.8) hold. Then, it holds that $c^H \mathcal{Q}(A) b = c^H \widehat{V} \mathcal{Q}(\widehat{W}^H A \widehat{V}) \widehat{W}^H b$ for any $\mathcal{Q}(\lambda) \in \mathbb{P}_{2l-1}(\lambda) / [\varphi(\lambda)\psi(\lambda)]$.*

Proof. Similar to Lemma 2.2, for the polynomial $\dot{\tau}_j(\lambda) := \dot{\alpha}_j^l \lambda^j + \dots + \dot{\alpha}_1^j \lambda + \dot{\alpha}_0^j$, we obtain

$$\begin{cases} \dot{\tau}_j(A) \varphi(A)^{-1} b = \widehat{V}_l \dot{\tau}_j(\widehat{T}_l) e_1, & j < l, \\ \dot{\tau}_l(A) \varphi(A)^{-1} b = \widehat{V}_l \dot{\tau}_l(\widehat{T}_l) e_1 + \dot{\alpha}_l^l \dot{\zeta}_l \widehat{v}_{l+1}, & j = l, \end{cases}$$

with $\dot{\zeta}_l = \widehat{\gamma}_{l+1} \cdots \widehat{\gamma}_3 \widehat{\gamma}_2$. Setting $\dot{\tau}_j(\lambda) = \varphi_{k_b}(\lambda)$, we obtain the following result:

$$\begin{cases} \varphi_{k_b}(A) \varphi_{k_b}(A)^{-1} b = \widehat{V}_l \varphi_{k_b}(\widehat{T}_l) e_1, & k_b < l, \\ \varphi_{k_b}(A) \varphi_{k_b}(A)^{-1} b = \widehat{V}_l \varphi_{k_b}(\widehat{T}_l) e_1 + \dot{\alpha}_l^l \dot{\zeta}_l \widehat{v}_{l+1}, & k_b = l, m_b = 0. \end{cases}$$

Note that $\widehat{W}_l^H \widehat{V}_l = I$, $\widehat{W}_l^H \widehat{v}_{l+1} = 0$ and $W^H \varphi(A)^{-1} b = e_1$. For either $k_b < l$ or $k_b = l$, it holds that

$$\begin{aligned}
\widehat{W}^H b &= \widehat{W}^H \varphi(A) \varphi(A)^{-1} b = \varphi(\widehat{T}_l) e_1 = \varphi(\widehat{T}_l) \widehat{W}^H \varphi(A)^{-1} b, \\
\varphi(\widehat{T}_l)^{-1} \widehat{W}^H b &= \widehat{W}^H \varphi(A)^{-1} b = e_1.
\end{aligned} \tag{2.16}$$

Similarly, we obtain

$$e_1 = \psi(\widehat{K}_l)^{-1} \widehat{V}^H c, \quad e_1^H = c^H \widehat{V} \psi(\widehat{K}_l)^{-H} = c^H \widehat{V} \psi(\widehat{T}_l)^{-1}. \tag{2.17}$$

The proof ends by rewriting Proposition 2.13 with (2.16) and (2.17). \square

For simple presentation, we assume that $\widehat{m}_0 = 1$, where $\widehat{m}_0 := c^H \psi(A)^{-1} \varphi(A)^{-1} b$. If $\widehat{m}_0 \neq 1$, then a similar discussion of Remark 2.6 can be applied. In a manner analogous to the treatment in [63], the linear functional with a weighted term is defined as follows.

$$\widehat{\mathcal{J}}(\mathcal{F}) := c^H \psi(A)^{-1} \mathcal{F}(A) \varphi(A)^{-1} b. \tag{2.18}$$

With the bases from (2.8), we have the Gauss-Christoffel quadrature formula:

$$\begin{aligned}
\widehat{\mathcal{J}}(\mathcal{F}) &= \widehat{\mathcal{J}}_G(\mathcal{F}) + \widehat{\mathcal{E}}(\mathcal{F}), \\
\text{i.e., } c^H \psi(A)^{-1} \mathcal{F}(A) \varphi(A)^{-1} b &= e_1^H \mathcal{F}(\widehat{T}_l) e_1 + \widehat{\mathcal{J}}([\Lambda(\lambda)]^2 \mathcal{F}[\lambda_1, \lambda_1, \lambda_2, \lambda_2, \dots, \lambda_l, \lambda_l, \lambda]).
\end{aligned} \tag{2.19}$$

As Proposition 2.13 shows, the equality $\widehat{\mathcal{J}}(\mathcal{P}) = \widehat{\mathcal{J}}_G(\mathcal{P})$ is satisfied for any $\mathcal{P}(\lambda) \in \mathbb{P}_{2l-1}$. It can thus be surmised that $\widehat{\mathcal{J}}_G(\mathcal{F}) = e_1^H \mathcal{F}(\widehat{T}_l) e_1$ represents the Gauss-Christoffel quadrature formula. After substituting $\widehat{\mathcal{H}}(\lambda, \mathfrak{s}) = \varphi(\lambda)\psi(\lambda)/(\mathfrak{s} - \lambda)$ into $\mathcal{F}(\lambda)$ in (2.19), we obtain the following quadrature remainder formula.

$$\begin{aligned} c^H \psi(A)^{-1} [\varphi(A)\psi(A)(\mathfrak{s}I - A)^{-1}] \varphi(A)^{-1} b &= e_1^H \psi(\widehat{T}_l)(\mathfrak{s}I - \widehat{T}_l)^{-1} \varphi(\widehat{T}_l) e_1 + \widehat{\mathfrak{E}}(\widehat{\mathcal{H}}), \\ c^H (\mathfrak{s}I - A)^{-1} b &= c^H \widehat{V}(\mathfrak{s}I - \widehat{W}^H A \widehat{V})^{-1} \widehat{W}^H b + \widehat{\mathfrak{E}}(\widehat{\mathcal{H}}), \end{aligned}$$

where $\varphi(\widehat{T}_l) e_1 = \widehat{W}^H b$ and $e_1^H \psi(\widehat{T}_l) = c^H \widehat{V}$ are described in (2.16) and (2.17), respectively. In conjunction with (2.14) and (2.18), we can derive the following form of the MOR error.

$$\begin{aligned} e(\mathfrak{s}) &= h(\mathfrak{s}) - \tilde{h}(\mathfrak{s}) = \widehat{\mathfrak{E}}(\widehat{\mathcal{H}}) = \widehat{\mathcal{J}}([\Lambda(\lambda)]^2 \widehat{\mathcal{H}}[\lambda_1, \lambda_1, \lambda_2, \lambda_2, \dots, \lambda_l, \lambda_l, \lambda]) \\ &= \left\{ \frac{\varphi(\mathfrak{s})\psi(\mathfrak{s})}{[\Lambda(\mathfrak{s})]^2} \right\} c^H \psi(A)^{-1} \Lambda(A) (\mathfrak{s}I - A)^{-1} \Lambda(A) \varphi(A)^{-1} b. \end{aligned} \quad (2.20)$$

We conclude by outlining the explanation with respect to variable λ . Proposition 2.12 represents the Hermitian interpolation formula. The integral is analogous to the linear functional with a weighted term (2.18). The Gauss-Christoffel quadrature formula is presented in (2.19). The Ritz values λ_i concern the interpolation and quadrature nodes. Propostion 2.13 and Propostion 2.14 reveal that Gauss quadrature has degree of precision $(2l - 1)$. Finally, the error formula $e(\mathfrak{s})$ corresponds to the Gauss quadrature remainder. More details can be found in the manuscript [51].

This section of the research is based on the fact that the Ritz values represent the quadrature nodes of a Gauss-Christoffel quadrature. This leads to the motivation to establish the relationship between the error formula and the moments matching. The book [50] by Liesen and Strakoš provides a comprehensive overview of the relationships among the symmetric Lanczos procedure ($A = A^H$ with $b = c$), moments matching, orthogonal polynomials, continued fractions and Gauss quadrature. Recently, Strakoš and his co-workers have a series of work on generalizing it onto the Lanczos biorthogonalization procedure [63–66, 72]. For further details on the Gauss quadrature, we refer the readers to [1, 15, 21, 23, 29, 35, 55, 69] and references therein.

2.5. The MOR error for the descriptor model: $E \neq I$. This section presents a discussion of the approximation of $h(\mathfrak{s}) = c^H (\mathfrak{s}E - A)^{-1} b$ by $\tilde{h}(\mathfrak{s}) = c^H \mathcal{V}(\mathfrak{s}W^H E \mathcal{V} - W^H A \mathcal{V})^{-1} W^H b$. For the sake of simplicity, we assume that E is invertible. Consequently, we obtain $h(\mathfrak{s}) = c^H [\mathfrak{s}I - (E^{-1}A)]^{-1} (E^{-1}b)$. Substituting it into Theorem 2.1, we obtain the error formula of MOR for the descriptor model.

$$\begin{aligned} \tilde{h}(\mathfrak{s}) &= c^H \mathcal{V}(\mathfrak{s} \widetilde{W}^H \mathcal{V} - \widetilde{W}^H E^{-1} A \mathcal{V})^{-1} \widetilde{W}^H (E^{-1}b) \\ &= c^H \mathcal{V}[\mathfrak{s}(E^{-H} \widetilde{W})^H E \mathcal{V} - (E^{-H} \widetilde{W})^H A \mathcal{V}]^{-1} (E^{-H} \widetilde{W})^H b \\ &= c^H \mathcal{V}(\mathfrak{s}W^H E \mathcal{V} - W^H A \mathcal{V})^{-1} W^H b, \end{aligned}$$

where \mathcal{V} and \widetilde{W} are set up by $(E^{-1}A, E^{-1}b, c)$ in Theorem 2.1. Later, we shall use $W = E^{-H} \widetilde{W}$ instead of \widetilde{W} .

THEOREM 2.15. *Let $\text{span}(\mathcal{V}) = \text{CK}(E^{-1}A, E^{-1}b, k_b, m_b)$ and $\text{span}(W) = \text{CK}((AE^{-1})^H, E^{-H}c, k_c, m_c)$ with $k_b + m_b = k_c + m_c =: l$. Suppose that the Lanczos biorthogonalization procedure of A , $[\prod_{j=2}^{k_b} (A - s_j E)^{-1} E](A - s_1 E)^{-1} b$ and $\prod_{j=2}^{k_c} (A - t_j E)^{-H} E^H](A - t_1 E)^{-H} c$ does not break down until the $(l + 1)$ th iteration. With notations (2.2) and (2.3), it holds that*

$$\begin{aligned} e(\mathfrak{s}) &= h(\mathfrak{s}) - \tilde{h}(\mathfrak{s}) = c^H (\mathfrak{s}E - A)^{-1} b - c^H \mathcal{V}(\mathfrak{s}W^H E \mathcal{V} - W^H A \mathcal{V})^{-1} W^H b \\ &= \frac{1}{g_b(\mathfrak{s})g_c(\mathfrak{s})} c^H g_c(E^{-1}A) (\mathfrak{s}I - E^{-1}A)^{-1} g_b(E^{-1}A) E^{-1} b \\ &= \frac{1}{g_b(\mathfrak{s})g_c(\mathfrak{s})} c^H g_c(E^{-1}A) g_b(E^{-1}A) (\mathfrak{s}E - A)^{-1} b, \end{aligned}$$

where $\Lambda(\lambda)$ is the monic characteristic polynomial of $(W^H E \mathcal{V})^{-1} W^H A \mathcal{V}$.

3. The error formula of the one-sided projection method. It is evident that the use of known methods can be applied to approximate $\mathcal{H}(A)b = (\mathfrak{s}I - A)^{-1}b$. It is the action of a matrix function on a vector, which is discussed in [42, Chapter 13] and [40, 41, 43]. Once the pre-multiplication by c^H has been performed, an approximation of the transfer function will be obtained. The basis is derived from the following:

$$\begin{aligned} \text{CK}(E^{-1}A, E^{-1}b, k, m) &:= \text{RK}(E^{-1}A, E^{-1}b, \mathbb{S}, k) \cup \text{Krylov}(E^{-1}A, E^{-1}b, m), \\ \text{span}(V_{2l}) &= \text{CK}(E^{-1}A, E^{-1}b, k, m) = \text{Krylov}(E^{-1}A, \varphi_k(E^{-1}A)^{-1}E^{-1}b, 2l), \\ V^H V &= I, \quad \varphi_k(\lambda) = \prod_{j=1}^k (\lambda - s_j), \quad k + m = 2l. \end{aligned} \tag{3.1}$$

By summarizing [10, (2.1)] and [22, (2.2)], we obtain the error of the one-sided projection method for MOR.

THEOREM 3.1. *Suppose the dimension of $\text{CK}(E^{-1}A, E^{-1}b, k, m)$ is $2l$. With notations (3.1), it holds that*

$$\begin{aligned} h(\mathfrak{s}) - \check{h}(\mathfrak{s}) &= c^H(\mathfrak{s}E - A)^{-1}b - c^H V(\mathfrak{s}V^H EV - V^H AV)^{-1}V^H b \\ &= \frac{1}{G_{\text{one}}(\mathfrak{s})} c^H G_{\text{one}}(E^{-1}A)(\mathfrak{s}E - A)^{-1}b, \end{aligned}$$

where

$$G_{\text{one}}(\lambda) := \frac{\bigwedge_{\text{one}}(\lambda)}{\varphi(\lambda)}, \tag{3.2}$$

with $\bigwedge_{\text{one}}(\lambda) = \prod_{i=1}^{2l} (\lambda - \lambda_i)$ be the monic characteristic polynomial of $(V^H EV)^{-1}V^H AV$.

We observe $G_{\text{one}}(\lambda)$ has a similar form to $G_{\text{two}}(\lambda)$ in (2.11), which is formed in the two-sided projection method. The primary difference is that the order of the reduced system obtained by the two-sided projection is l , while the one-sided projection yields $2l$. In comparison to the numerical quadrature, it is readily comprehensible. To attain the degree of precision $2l - 1$, it is possible to employ Gauss quadrature (two-sided projection method, cf. Section 2.4.2), or alternatively, to utilize an interpolating polynomial of degree $2l - 1$ to perform the integral (one-sided projection method, cf. Section 3). This phenomenon has also been observed in numerical experiments (cf. Section 6).

4. Interpolatory H_∞ norm MOR. In this section, we assume A is c -stable, which implies that the eigenvalues of A are located on left-hand half plane. The norm $\|\cdot\|_{H_\infty}$ is defined in a \mathcal{H}_∞ -space. The space requires the function matrix to be analytic and bounded in the open right-hand half plane. For $h(\mathfrak{s}) \in \mathcal{H}_\infty^n$, we have $\|h(\mathfrak{s})\|_{H_\infty} = \sup_{\mathfrak{s} \in i\mathbb{R} \cup \{\infty\}} |c^H(\mathfrak{s}I - A)^{-1}b|$. The MOR in the H_∞ norm sense is to solve the optimization problem:

$$\|h(\mathfrak{s}) - \hat{h}_*(\mathfrak{s})\|_{H_\infty} = \min_{\hat{h}(\mathfrak{s}) \in \mathcal{H}_\infty^l} \|h(\mathfrak{s}) - \hat{h}(\mathfrak{s})\|_{H_\infty}, \tag{4.1}$$

$$\begin{aligned} \text{where } h(\mathfrak{s}) &= c^H(\mathfrak{s}E - A)^{-1}b, \\ \hat{h}(\mathfrak{s}) &= c_l^H(\mathfrak{s}E_l - A_l)^{-1}b_l + d_l. \end{aligned} \tag{4.2}$$

The motivation of the H_∞ norm MOR is clearly described in [25, Section 1]. More theories and algorithms can be found in [37, 44] and references therein. It is worth noting that balanced truncation methods [57, 58] provide an H_∞ norm estimation of the model error by using the Hankel singular values [2, 56].

We approximately solve (4.1) by solving the interpolatory H_∞ norm MOR. Concretely speaking, the function $\hat{h}(\mathfrak{s})$ in (4.1) is constrained to be equal to $\check{h}(\mathfrak{s})$, which is an interpolatory transfer function. Therefore, the reduced transfer function $\check{h}(\mathfrak{s})$ is a rational interpolating function of $h(\mathfrak{s})$. This implies that $\check{h}(\mathfrak{s})$ can be formed by a rational Krylov subspaces projection method. For simplicity, we shall set $d_l = 0$. As the order l increases, the error $\|h(\mathfrak{s}) - \check{h}(\mathfrak{s})\|_{H_\infty}$ decreases.

In seeking the optimal shifts for $\tilde{h}(\mathfrak{s})$, it is evident that the shifts must fully influence the error $e(\mathfrak{s})$. Hence, we set $k_b = k_c = l$. In the words of finding the optimal shifts, the interpolatory H_∞ norm MOR can be expressed as the following optimization problem.

$$\begin{aligned} \min_{s_1, s_2, \dots, s_l, t_1, t_2, \dots, t_l} \sup_{\mathfrak{s} \in i\mathbb{R} \cup \{\infty\}} |e(\mathfrak{s})| &= \min_{s_1, s_2, \dots, s_l, t_1, t_2, \dots, t_l} \sup_{\mathfrak{s} \in i\mathbb{R} \cup \{\infty\}} |h(\mathfrak{s}) - \tilde{h}(\mathfrak{s})| \\ &= \min_{s_1, s_2, \dots, s_l, t_1, t_2, \dots, t_l} \sup_{\mathfrak{s} \in i\mathbb{R} \cup \{\infty\}} \left| \frac{1}{G(\mathfrak{s})} \right| |c^H G(E^{-1}A)(\mathfrak{s}E - A)^{-1}b|, \end{aligned} \quad (4.3)$$

where $G(\mathfrak{s})$ is either $G_{\text{two}}(\mathfrak{s})$ in (2.11) or $G_{\text{one}}(\mathfrak{s})$ in (3.2). Given that $(\mathfrak{s}E - A)$ is an $n \times n$ matrix, the complete computation of $e(\mathfrak{s})$ is time-consuming. Consequently, the development of effective algorithms demands the utilization of certain approximations of $e(\mathfrak{s})$.

REMARK 4.1. *We establish the following approximations for $|e(\mathfrak{s})|$.*

$$\begin{aligned} e(\mathfrak{s}) &= h(\mathfrak{s}) - \tilde{h}(\mathfrak{s}) = \frac{1}{G(\mathfrak{s})} c^H G(E^{-1}A)(\mathfrak{s}E - A)^{-1}b, \\ \text{Approximation 1: } |e(\mathfrak{s})| &\approx \mathcal{C}_1 \frac{1}{|G(\mathfrak{s})|}, \\ \text{Approximation 2: } |e(\mathfrak{s})| &\leq \frac{1}{|G(\mathfrak{s})|} \|c^H G(E^{-1}A)\|_2 \|(\mathfrak{s}E - A)^{-1}b\|_2 \\ &\approx \frac{1}{|G(\mathfrak{s})|} \mathcal{C}_2 \|V(\mathfrak{s}W^H EV - W^H AV)^{-1}W^H b\|_2 \\ &= \mathcal{C}_2 \frac{1}{|G(\mathfrak{s})|} \|(\mathfrak{s}W^H EV - W^H AV)^{-1}W^H b\|_2. \end{aligned}$$

The term $G(\mathfrak{s})$ is a quantity formula, which implies that it can be computed easily. The one-sided projection algorithm in [22] is designed by using Approximation 1 (cf. Algorithm 1). Except $1/G(\mathfrak{s})$, the left of $e(\mathfrak{s})$ is still dependent on \mathfrak{s} . This implies that Approximation 1 can be improved. In Approximation 2, we employ $\|V(\mathfrak{s}W^H EV - W^H AV)^{-1}W^H b\|_2$ to approximate $\|(\mathfrak{s}E - A)^{-1}b\|_2$. In our experimental examples (cf. Table 6.1), it can be observed that algorithms based on Approximation 2 exhibit better behaviour than those based on Approximation 1.

5. Greedy algorithms for MOR. As outlined in the books [2, 14], a range of methodologies exists for MOR. In the field of rational Krylov subspace projection methods, there exist numerous adaptive algorithms based on various error estimations [6, 7, 26, 27, 62]. By using Remark 4.1, we propose a greedy two-sided projection algorithm, which is a modification of a one-sided projection algorithm in [22].

5.1. Algorithm ARKSM. In paper [22], it is required that the shifts should be either real numbers or conjugate pairs. For simplicity, we do not impose this constraint. The one-sided projection algorithm is outlined in Algorithm 1. The concept of the greedy algorithm is employed in (5.1) for computing the optimal shifts. As stated in Remark 4.1 Approximation 1, the error $|e(\mathfrak{s})|$ is actually approximated by $\mathcal{C}_1/|G(\mathfrak{s})|$. The initial two shifts are acquired by

$$s_{\min} = \text{eigs}(-A, E, 1, 'sm'), \quad s_{\max} = \text{eigs}(-A, E, 1, 'lm'). \quad (5.2)$$

The other shifts are selected on the boundary of Ξ , which is a mirror region of the Ritz values. The designation of Ξ is based on the observation that the optimal H_2 norm MOR condition is $s_i = -\bar{\lambda}_i$ [39]. By applying the maximal value theorem to Ξ , one can ascertain that the shifts are located on the boundary $\partial\Xi$. Another explanation can be found in [41, Section 4.1].

Algorithm 1 Adaptive Rational Krylov Subspace Method (ARKSM) for MOR [22]**Input:** $A, E \in \mathbb{C}^{n \times n}, b, c \in \mathbb{C}^{n \times 1}$.**Input:** $s_{\min}, s_{\max}, l_{\max}$.

- 1: $s_1 = s_{\min}, v_1 = (A - s_1 E)^{-1} b$;
- 2: $s_2 = s_{\max}, v_2 = (A - s_2 E)^{-1} b$;
- 3: $V = [v_1, v_2]; \quad V = \text{orth}(V)$;
- 4: **for** $l = 2, \dots, l_{\max}$ **do**
- 5: Update $V^H A V; V^H E V; V^H b$;
- 6: Get Ritz values $\lambda_i \in \text{eig}((V^H E V)^{-1} V^H A V)$;
- 7: Determine $\partial \Xi = \text{convex hull of } \{-\lambda_1, \dots, -\lambda_l, s_{\min}, s_{\max}\}$;
- 8: Select the next shift s_{l+1} :

$$s_{l+1} = \arg \max_{\mathfrak{s} \in \partial \Xi} \left| \frac{\prod_{j=1}^l (\mathfrak{s} - s_j)}{\prod_{j=1}^l (\mathfrak{s} - \lambda_j)} \right|. \quad (5.1)$$

9: $v_{l+1} = (A - s_{l+1} E)^{-1} b$;10: $V = \text{orth}([V, v_{l+1}])$;11: **end for****Output:** V ; Shifts $s_l (l = 1, 2, \dots, l_{\max})$; $\check{h}(\mathfrak{s}) = c^H V(\mathfrak{s} V^H E V - V^H A V)^{-1} V^H b \approx h(\mathfrak{s})$.

5.2. Two-sided algorithms. We propose the greedy two-sided algorithm in Algorithm 2. Since $E^{-1}A$ is c -stable, it is preferable to utilize shifts on the right half-plane in order to guarantee that $(A - s_i E)$ remains nonsingular. The boundary of the right half plane is the imaginary axis. Moreover, we are currently doing research on H_∞ norm MOR, which is defined on the imaginary axis. Thus, we shall select the shifts on the imaginary axis. Selecting shifts along the imaginary axis is a non-novel operation (e.g. [26, 27]). In practice, our shifts are selected on $\mathbb{Z}(\alpha, \beta, 500)$, where

$$\mathbb{Z}(\alpha, \beta, k) = [-\iota \times \text{logspace}(\alpha, \beta, k), 0, \iota \times \text{logspace}(\alpha, \beta, k)]. \quad (5.4)$$

In the two-sided algorithm, the function $G(\mathfrak{s})$ is $G_{\text{two}}(\mathfrak{s})$ in (2.11). Since the variable \mathfrak{s} in $e(\mathfrak{s})$ is actually independent of the obtained shifts and Ritz values, the greedy algorithm is an appropriate method for solving (4.3). The next shifts are obtained by identifying the maximal point of the current error. On Line 9, we provide two potential options for the next shift, which correspond to the approximations of $e(\mathfrak{s})$ in Remark 4.1.

Moreover, we claim that the obtained shifts are distinct, given that any obtained shifts satisfy $e(s_j) = 0$, which implies that they cannot be the maximal points of the error. In other words, the shifts obtained will not be selected in the subsequent iterations. This fact implies that we can orthogonalize $[V, (A - s_i E)^{-1} b]$ instead of $[V, (A - s_i E)^{-1} v]$, where v is the last vector of V . This is the process that is undertaken on Line 12.

The computation of (5.3) is inexpensive. The computation of $\varphi_l(\mathfrak{s}), \psi_l(\mathfrak{s})$ and $\Lambda(\mathfrak{s})$ merely involves quantity calculations. In order to implement Option 2, it is necessary to solve the following small order linear equations: $(\mathfrak{s} W^H E V - W^H A V)^{-1} V^H b$. All of the coefficient matrices are identical, while only \mathfrak{s} varies in \mathbb{Z}_2 . Consequently, we are able to utilize `hess(WHEV, WHAV)` and `linsolve(..., opts.UHES=1)` to reduce the CPU time.

A challenge is presented in determining the value of t_{l+1} for the left subspace. A simple decision is made by setting $t_{l+1} = \overline{s_{l+1}}$. A number of alternative strategies regarding t_{l+1} have been investigated, which are analogous to the previously discussed strategies concerning s_{l+1} . The results of our numerical testing do not indicate that those options exhibit better behaviors than the proposed strategy of $t_{l+1} = \overline{s_{l+1}}$.

Algorithm 2 Two-sided greedy rational Krylov subspace method for MOR

Input: $A, E \in \mathbb{C}^{n \times n}, b, c \in \mathbb{C}^{n \times 1}$.

Input: $\alpha, \beta, k_{\text{two}}, s_{\text{max}}, l_{\text{max}}$, Option number in (5.3).

- 1: $s_1 = |s_{\text{max}}|t/10, v_1 = (A - s_1 E)^{-1}b$;
- 2: $t_1 = -|s_{\text{max}}|t/10, w_2 = (A - s_2 E)^{-H}c$;
- 3: $V = \text{orth}(v_1); W = \text{orth}(w_1)$;
- 4: Determine the set for choosing shifts: $\mathbb{Z}_2 = \mathbb{Z}(\alpha, \beta, k_{\text{two}})$ from (5.4);
- 5: **for** $l = 1, \dots, l_{\text{max}}$ **do**
- 6: Update $W^H AV; W^H EV; W^H b; c^H V$;
- 7: Get Ritz values $\lambda_i \in \text{eig}((W^H EV)^{-1}W^H AV)$; $\Lambda(\mathfrak{s}) := \prod_{i=1}^l (\mathfrak{s} - \lambda_i)$;
- 8: Set new symbols: $\varphi_l(\mathfrak{s}) := \prod_{i=1}^l (\mathfrak{s} - s_i)$; $\psi_l(\mathfrak{s}) := \prod_{i=1}^l (\mathfrak{s} - t_i)$;
- 9: Select next shift for s_{l+1} :

$$\begin{aligned}
 \text{Option 1: } \quad s_{l+1} &= \arg \max_{\mathfrak{s} \in \mathbb{Z}_2} \left| \frac{\varphi_l(\mathfrak{s})\psi_l(\mathfrak{s})}{[\Lambda(\mathfrak{s})]^2} \right|, \\
 \text{Option 2: } \quad s_{l+1} &= \arg \max_{\mathfrak{s} \in \mathbb{Z}_2} \left| \frac{\varphi_l(\mathfrak{s})\psi_l(\mathfrak{s})}{[\Lambda(\mathfrak{s})]^2} \right| \|(\mathfrak{s}W^H EV - W^H AV)^{-1}W^H b\|_2,
 \end{aligned} \tag{5.3}$$

- 10: Select the next shift for t_{l+1} :

$$t_{l+1} = \text{conj}(s_{l+1});$$

- 11: $v_{l+1} = (A - s_{l+1}E)^{-1}b; w_{l+1} = (A - t_{l+1}E)^{-H}c$;
- 12: $V = \text{orth}([V, v_{l+1}]); W = \text{orth}([W, w_{l+1}])$;
- 13: **end for**

Output: $V, W, \tilde{h}(\mathfrak{s}) = c^H V(\mathfrak{s}W^H EV - W^H AV)^{-1}W^H b \approx h(\mathfrak{s})$.

The H_∞ norm error is quantified by the max error:

$$\|e(\mathfrak{s})\|_\infty = \max_{\mathfrak{s} \in \mathbb{Z}_e} |h(\mathfrak{s}) - \tilde{h}(\mathfrak{s})|, \tag{5.5}$$

where \mathbb{Z}_e also has form (5.4). Our greedy algorithms actually are not required to compute it. The max error is employed only for the purpose of evaluation in comparison with other algorithms. The computation of the max error requires a significant amount of calculation. This is not analogous to the case of matrix equations, where the residual norm can be computed in the reduced problems [52, 53].

6. Numerical experiments. All experiments are carried out in Matlab2016a on a notebook computer (64 bits) with an Intel CPU i7-5500U and 8GB memory. Any data involving random numbers are fixed by setting `rand('state', 0)` or `randn('state', 0)`. It is worthy of mention that `eigs` employs a random vector as the initial vector. Prior to utilizing `eigs` for computing (5.2), we also set `rand('state', 0)`. We shall compare our greedy algorithms with ARKSM (Algorithm 1), the adaptive Antoulas-Anderson (AAA) algorithm and the iterative rational Krylov algorithm (IRKA).

The AAA algorithm can be applied for MOR [3, 24, 59]. As it is designed to solve a minimum-maximum problem, it can therefore be considered to approximately solve the H_∞ norm MOR problem (4.1). The algorithm acquires samples along the imaginary axis [59, Section 6.9]. The greedy idea is also employed, resulting in the selected samples being nested. In the testing procedure, the samples set \mathbb{Z}_A are constructed to have the same form of $\mathbb{Z}(\alpha, \beta, k)$. When $\mathbb{Z}_A = \mathbb{Z}_e$ is set, the max error is directly outputted by AAA. This is an attractive advantage of the AAA algorithm.

The H_2 norm optimal MOR is accomplished by IRKA [9, 39]. When IRKA converges, the optimal shifts are obtained, which satisfy the condition that $t_i = s_i = -\bar{\lambda}_i$. The same shifts are used for spanning the left and

right rational Krylov subspaces. The projection process reveals that H_2 norm optimal MOR is also a two-sided projection method. Therefore, its error $e(\mathfrak{s})$ can be expressed by Theorem 2.1. The two main disadvantages of IRKA are as follows: The convergence rate is relatively slow, and the optimal shifts are not nested with respect to order l . The advantage is that it has an optimization property in the H_2 norm sense. It is not necessary for IRKA to compute the model error in either the H_2 or the H_∞ norm, as this is automatically optimized in the H_2 norm sense. Nonetheless, we continue to employ its max error (5.5) as an applicable standard for comparison with other algorithms. The initial shifts of IRKA are derived from the output shifts of ARKSM. The IRKA iteration is terminated if the iteration number exceeds 100 or if the condition $\|S_j - S_{j-1}\|_2 < 10^{-6}\|S_j\|_2$ is satisfied, where S_j represents the sorted shifts vector at the j th iteration.

For large-scale problems, the computation of all algorithms is primarily focused on the process of solving linear equations. In all tests, the Matlab `backslash` function is directly employed to complete the calculations of both $(A - s_i E)^{-1}b$ and $(A - s_i E)^{-H}c$. In the case of an l -order MOR, the number of linear solvers required for each algorithm is taken into account. The AAA algorithm requires the sampling of $h(\mathfrak{s})$ on the imaginary axis. The function $h(\mathfrak{s})$ is evaluated for $\mathfrak{s} \in \mathbb{Z}_A = \mathbb{Z}(\alpha_A, \beta_A, k_A)$. Therefore, it requires a total of $(2k_A + 1)$ linear solvers, which is independent of the order l . The IRKA algorithm requires $2j_{\max}l$ linear solvers, where j_{\max} represents the final iteration number at which the algorithm terminates. The ARKSM algorithm requires l linear solvers, whereas our two-sided algorithm requires $2l$ linear solvers. Note that ARKSM is a one-sided type of projection algorithm. By contrast, both H_2 (IRKA) and our greedy two-sided algorithm are two-sided types.

Example 1 (small problems): The testing examples are taken from the SLICOT benchmark problems [13, 19]. In instances wherein the model problems possess both multiple inputs and outputs, we set $\mathbf{b}=\mathbf{B}(:,1)$ and $\mathbf{c}=\mathbf{C}(1,:)$. We set $\mathbb{Z}_e = \mathbb{Z}_A = \mathbb{Z}(-3, 5, 700)$ for computing the max error and undertaking sampling in AAA. In two-sided algorithms., the shifts are selected in $\mathbb{Z}_2 = \mathbb{Z}(-3, 5, 500)$.

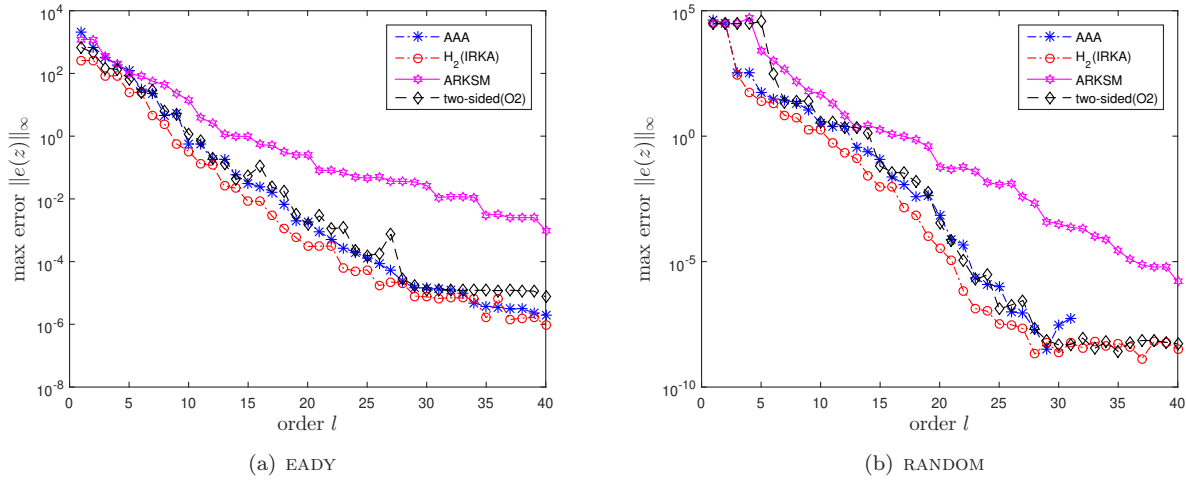
Table 6.1: 40-order MOR of small problems

| | Matrix | BEAM | CDPLAYER | EADY | FOM | ISS | RANDOM |
|------------------------------|---------------|----------|----------|----------|----------|----------|----------|
| | Size | 348 | 120 | 598 | 1006 | 270 | 200 |
| CPU(s) | Sampling | 7.08 | 0.20 | 40.13 | 0.51 | 0.40 | 3.76 |
| | AAA | 7.67 | 0.72 | 40.66 | 0.80 | 1.01 | 4.11 |
| | ARKSM | 2.96 | 2.62 | 3.87 | 2.67 | 2.64 | 2.91 |
| | two-sided(O1) | 3.21 | 2.72 | 5.61 | 2.92 | 2.84 | 3.04 |
| | two-sided(O2) | 5.02 | 4.72 | 7.03 | 4.61 | 4.60 | 4.79 |
| | H_2 (IRKA) | 44.85 | 0.78 | 235.87 | 4.18 | 2.02 | 23.60 |
| $\ e(\mathfrak{s})\ _\infty$ | AAA | 5.83E-02 | 2.29E-03 | 2.28E-06 | 5.96E-12 | 4.54E-06 | 1.21E-09 |
| | ARKSM | 1.29E+01 | 3.87E+01 | 9.88E-04 | 5.01E-12 | 4.05E-03 | 1.61E-06 |
| | two-sided(O1) | 1.12E+00 | 1.02E-01 | 1.58E-05 | 1.02E-11 | 4.26E-05 | 6.67E-09 |
| | two-sided(O2) | 6.76E-01 | 9.25E-02 | 7.51E-06 | 3.72E-12 | 2.68E-05 | 5.25E-09 |
| | H_2 (IRKA) | 4.24E-02 | 2.49E-02 | 9.77E-07 | 4.32E-12 | 1.57E-05 | 3.18E-09 |
| | IRKA#iter | 100 | 39 | 100 | 100 | 62 | 100 |

The ‘‘sampling’’ stage concerns the CPU times associated with the evaluation of $h(\mathfrak{s})$ for $\mathfrak{s} \in \mathbb{Z}_A = \mathbb{Z}_e = \mathbb{Z}(-3, 5, 700)$. As illustrated in Fig. 6.1, the data of AAA is only concerned with $l = 29$ for FOM and $l = 31$ for RANDOM. In this table, the H_2 norm MOR(IRKA) is not computed for $l < 40$. The initial shifts of IRKA are obtained from the output shifts of the ARKSM algorithm. The term ‘‘IRKA#iter’’ denotes the iteration number of IRKA at the point of termination.

Two error images are presented in Fig. 6.1, while the CPU times for 40-order MOR are listed in Table 6.1. With the exception of the H_2 norm optimal MOR (IRKA), the remaining algorithms employ nested shifts. Hence, their Matlab codes for producing Fig. 6.1 and Table 6.1 exhibit minimal discrepancies. However, only the 40-order H_2 norm optimal MOR is computed in Table 6.1, while the H_2 norm optimal MOR of all orders ($l = 1, 2, \dots, 40$) is computed in Figure 6.1.

Fig. 6.1: Behaviors of different MOR for small problems



Despite inputting $l = 40$ into the AAA algorithm, the process terminates at $l = 31$ for RANDOM.

Example 2 (large-scale problems): With $E = I$, the problems L10000 and L10648 respectively originate from papers [22] and [70]. They are derived from the explicit discretisation of partial differential equations. The remaining problems originate from the Oberwolfach collection [46]. A summary of the remaining information can be found in the first section of Table 6.2.

We set $\mathbb{Z}_A = \mathbb{Z}_e = \mathbb{Z}(\alpha, \beta, 400)$ and $\mathbb{Z}_2 = \mathbb{Z}(\alpha, \beta, 500)$. Two error images are presented in Fig. 6.2, while the CPU times for 40 order MOR are listed in Table 6.2. The remaining settings are identical to those previously described for small problems.

Fig. 6.2: Behaviors of different MOR for large-scale problems

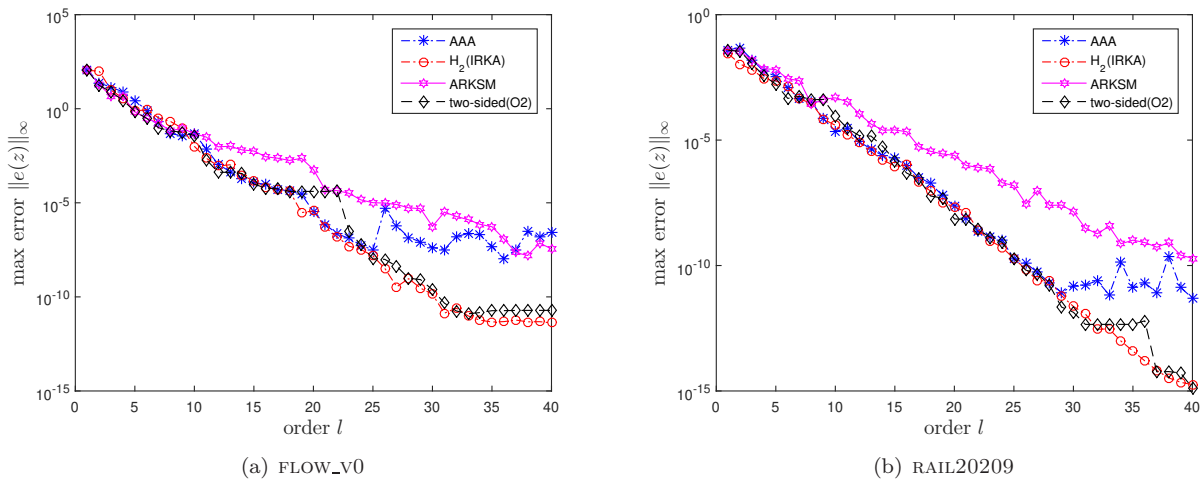


Table 6.2: 40-order MOR of large scale problems

| | Matrix | L10000 | L10648 | FLOW_v0 | FLOW_v0.5 | RAIL5177 | RAIL20209 |
|------------------------------|-----------------|-------------------------|-------------------------|----------------------|----------------------|----------------------|----------------------|
| Info. | Size | 10000 | 10648 | 9669 | 9669 | 5177 | 20209 |
| | symmetry | No | No | Yes | No | Yes | Yes |
| | b | <code>ones(n,1)</code> | <code>ones(n,1)</code> | <code>B(:,1)</code> | <code>B(:,1)</code> | <code>B(:,6)</code> | <code>B(:,6)</code> |
| | c | <code>randn(n,1)</code> | <code>randn(n,1)</code> | <code>C(4,:)'</code> | <code>C(1,:)'</code> | <code>C(2,:)'</code> | <code>C(2,:)'</code> |
| | α, β | -2,5 | -3,4 | -1,8 | -3,5 | -6,3 | -6,3 |
| CPU(s) | Sampling | 57.94 | 323.14 | 70.04 | 68.99 | 24.10 | 113.42 |
| | AAA | 58.24 | 323.47 | 70.37 | 69.34 | 24.48 | 113.81 |
| | ARKSM | 6.21 | 20.25 | 4.49 | 6.15 | 2.71 | 6.81 |
| | two-sided(O1) | 9.81 | 41.37 | 11.68 | 15.30 | 5.31 | 19.04 |
| | two-sided(O2) | 12.16 | 42.38 | 13.31 | 29.22 | 7.08 | 21.18 |
| | H_2 (IRKA) | 120.56 | 1073.56 | 671.25 | 682.88 | 254.41 | 1106.58 |
| $\ e(\mathfrak{s})\ _\infty$ | AAA | 1.6E-06 | 2.2E-06 | 8.3E-08 | 7.9E-09 | 2.5E-12 | 6.5E-11 |
| | ARKSM | 2.2E-02 | 8.9E-04 | 3.6E-08 | 1.5E-05 | 4.6E-10 | 1.9E-10 |
| | two-sided(O1) | 8.0E-06 | 3.8E-06 | 1.3E-08 | 5.9E-12 | 6.8E-16 | 1.3E-15 |
| | two-sided(O2) | 4.3E-06 | 1.6E-05 | 1.9E-11 | 2.5E-12 | 6.4E-16 | 1.3E-15 |
| | H_2 (IRKA) | 1.5E-07 | 9.7E-07 | 4.2E-12 | 3.0E-10 | 8.6E-16 | 1.8E-15 |
| | IRKA#iter | 21 | 32 | 100 | 100 | 100 | 100 |

The vectors b and c of the RAIL20209 model are presented in [39, Section 5.3]. In accordance with (5.2), 10^α identified as a lower bound of $|s_{\min}|$, and thus, 10^β is established as an upper bound of $|s_{\max}|$. The ‘‘sampling’’ stage concerns the CPU times associated with the evaluation of $h(\mathfrak{s})$ for $\mathfrak{s} \in \mathbb{Z}_A = \mathbb{Z}_e = \mathbb{Z}(\alpha, \beta, 400)$. We set $\mathbb{Z}_2 = \mathbb{Z}(\alpha, \beta, 500)$ for the two-sided algorithm. The remaining settings are identical to those previously described in Table 6.1.

The following observations are presented for consideration.

1. The data presented in Tables 6.1 and 6.2 clearly demonstrate that the CPU times associated with the sampling process constitute a significant proportion of the overall processing time for the AAA algorithm. As the sampling process is not a necessary step in the execution of other algorithms, the CPU times involved in sampling are not incorporated into their respective computations. Nevertheless, we continue to perform sampling for computing the max error (5.5), so that all of the algorithms can be compared according to the same criteria.
2. As illustrated in Fig.6.2, the error images produced by the two-sided(O2) algorithm are comparable to those generated by the H_2 norm MOR and AAA. Given that the H_2 norm MOR exhibits H_2 norm optimality and that the effectiveness of AAA is already demonstrated in numerous examples [59], it can be stated that our greedy algorithms developed for solving the H_∞ norm MOR demonstrate favourable behavior. Meanwhile, our two-sided(O2) algorithm requires a much shorter processing time than IRKA and AAA in dealing with large-scale problems.
3. Both the H_2 norm optimal MOR (IRKA) and our greedy two-sided algorithm are two-sided type projection methods. A total of 80 shifts have been allocated for a 40-order MOR. In comparison, the ARKSM algorithm is, in fact, a one-sided type projection method. For a 40-order MOR, only 40 shifts are permitted in ARKSM. In Section 3, it is revealed that the forms of the errors associated with the l -order two-sided method and the $2l$ -order one-sided method are strikingly analogous. It is thus proposed that the 20-order two-sided algorithm will demonstrate a similar level of precision to that exhibited by the 40-order one-sided algorithm. The error pictures in Fig.6.1 and Fig.6.2 illustrate this phenomenon to some extent, as evidenced by the EADY, RANDOM and RAIL20209 examples. Concretely speaking, the max error of $l = 40$ in ARKSM is approximately equivalent to that of $l = 20$ in H_2 (IRKA) or the two-sided algorithm.

7. Conclusion. The following is a summary of the contributions.

1. We derive an explicit error formula for MOR, when MOR is accomplished by rational Krylov subspace methods. The moments matching results of MOR are particular cases of our error formula.
2. In the field of numerical analysis, the error formula is a valuable tool for theoretical analysis. We obtain two explanations of $e(\mathfrak{s})$, regarding the variables \mathfrak{s} and λ in the resolvent function $\mathcal{H}(\lambda, \mathfrak{s}) = 1/(\mathfrak{s} - \lambda)$. With respect to \mathfrak{s} , we observe that $h(\mathfrak{s})$ represents the interpolated function, $\tilde{h}(\mathfrak{s})$ represents the rational interpolating function, and the model error $e(\mathfrak{s})$ is given by the Hermitian interpolation remainder.
3. In the situation regarding λ , the function $\hat{\mathcal{H}}(\lambda) = \varphi(\lambda)\psi(\lambda)/(\mathfrak{s} - \lambda)$ has a non-relevant parameter \mathfrak{s} . The integral is now expressed by the linear functional with a weighted term (2.18). We demonstrate that $h(\mathfrak{s})$ represents the integral of $\hat{\mathcal{H}}(\lambda)$, that $\tilde{h}(\mathfrak{s})$ represents the Gauss-Christoffel quadrature formula, and that the model error $e(\mathfrak{s})$ is, in fact, the quadrature remainder.
4. A thorough examination of the form of the errors reveals a similarity between the errors in $2l$ -order one-sided projection methods and those in l -order two-sided projection methods. The numerical experiments also demonstrate this similarity.
5. We obtain an affordable approximation of $e(\mathfrak{s})$, which can be computed in the reduced problem. By using the approximation, we propose a greedy two-sided projection method for the interpolatory H_∞ norm MOR. The efficiency of the algorithm is evidenced by numerical experiments.

We explain two documented phenomena. 1. The error formula is independent of the stability of the system. Consequently, the projection methods are incapable of preserving the stability unless additional constraints are introduced. 2. The final error formula is independent of the bases in rational Krylov subspaces. For numerical stability, the researchers have elected to utilize the orthonormal bases in both left and right subspaces.

A challenge arises in attempting to generalize the error formula to a multi-input-multi-output system. Once the concise and explicit expressions of the residuals have been obtained, the error formula of the full interpolation [4, Section 3.3] can be obtained by $e(\mathfrak{s}) = R_C^H(\mathfrak{s}I - A)^{-1}R_B$. While [30, Theorem 4.3] describes certain properties of the residuals, there is still a need for a more concise expression. Another technical challenge is the utilization of tangential interpolation. Once the left and right tangential directions have been fixed by setting $c = c_i$ and $b = b_i$ (cf. [4, Theorem 3.3.1, Theorem 3.3.2]), the error formula can be readily rewritten, involving only A , Bb and Cc . The issue of how to express the error formula concisely when considering different left and right tangential directions remains unresolved.

Acknowledge. The author deeply appreciates Valeria Simoncini, Ren-cang Li and Shengxin Zhu for their insightful comments.

REFERENCES

- [1] J. ALAHMADI, M. PRANIĆ, AND L. REICHEL, *Rational Gauss quadrature rules for the approximation of matrix functionals involving Stieltjes functions*, Numer. Math., 151 (2022), pp. 443–473.
- [2] A. C. ANTOULAS, *Approximation of large-scale dynamical systems*, vol. 6 of Advances in Design and Control, Society for Industrial and Applied Mathematics (SIAM), Philadelphia, PA, 2005.
- [3] A. C. ANTOULAS AND B. D. Q. ANDERSON, *On the scalar rational interpolation problem*, IMA Journal of Mathematical Control and Information, 3 (1986), pp. 61–88.
- [4] A. C. ANTOULAS, C. A. BEATTIE, AND S. GUGERCIN, *Interpolatory Methods for Model Reduction*, Society for Industrial and Applied Mathematics, Philadelphia, PA, 2020.
- [5] Z. BAI AND Y. SU, *Dimension reduction of large-scale second-order dynamical systems via a second-order Arnoldi method*, SIAM J. Sci. Comput., 26 (2005), pp. 1692–1709.
- [6] H. BARKOUI, A. H. BENTBIB, AND K. JBILOU, *An adaptive rational block Lanczos-type algorithm for model reduction of large scale dynamical systems*, J. Sci. Comput., 67 (2016), pp. 221–236.
- [7] ———, *A matrix rational Lanczos method for model reduction in large-scale first- and second-order dynamical systems*, Numer. Linear Algebra Appl., 24 (2017), pp. e2077, 13.
- [8] U. BAUR, P. BENNER, AND L. FENG, *Model order reduction for linear and nonlinear systems: a system-theoretic perspective*, Arch. Comput. Methods Eng., 21 (2014), pp. 331–358.
- [9] C. BEATTIE, Z. DRMAČ, AND S. GUGERCIN, *Revisiting IRKA: Connections with Pole Placement and Backward Stability*, Vietnam J. Math., 48 (2020), pp. 963–985.

- [10] B. BECKERMANN, *An error analysis for rational Galerkin projection applied to the Sylvester equation*, SIAM J. Numer. Anal., 49 (2011), pp. 2430–2450.
- [11] P. BENNER, A. COHEN, M. OHLBERGER, AND K. WILLCOX, eds., *Model reduction and approximation: theory and algorithms*, vol. 15 of Computational Science & Engineering, Society for Industrial and Applied Mathematics (SIAM), Philadelphia, PA, 2017.
- [12] P. BENNER, S. GUGERCIN, AND K. WILLCOX, *A survey of projection-based model reduction methods for parametric dynamical systems*, SIAM Rev., 57 (2015), pp. 483–531.
- [13] P. BENNER, V. MEHRMANN, V. SIMA, S. VAN HUFFEL, AND A. VARGA, *SLICOT—a subroutine library in systems and control theory*, in Applied and computational control, signals, and circuits, Vol. 1, vol. 1 of Appl. Comput. Control Signals Circuits, Birkhäuser Boston, Boston, MA, 1999, pp. 499–539.
- [14] P. BENNER, V. MEHRMANN, AND D. C. SORENSEN, eds., *Dimension reduction of large-scale systems*, vol. 45 of Lecture Notes in Computational Science and Engineering, Springer, Berlin, 2005.
- [15] A. H. BENTBIB, M. EL GHOMARI, K. JBILOU, AND L. REICHEL, *The extended symmetric block Lanczos method for matrix-valued Gauss-type quadrature rules*, J. Comput. Appl. Math., 407 (2022), pp. Paper No. 114037, 18.
- [16] M. BERLJafa, S. ELSWORTH, AND S. GÜTTEL, *A rational krylov toolbox for matlab*, (2014).
- [17] R. L. BURDEN AND J. D. FAIRES, *Numerical analysis(9th edition)*, Prindle, Weber & Schmidt, Boston, Mass., 2010.
- [18] C. CARTIS, N. I. M. GOULD, AND P. L. TOINT, *Adaptive cubic regularisation methods for unconstrained optimization. Part I: motivation, convergence and numerical results*, Math. Program., 127 (2011), pp. 245–295.
- [19] Y. CHAHLAOUI AND P. VAN DOOREN, *Benchmark examples for model reduction of linear time-invariant dynamical systems*, in Dimension reduction of large-scale systems, vol. 45 of Lect. Notes Comput. Sci. Eng., Springer, Berlin, 2005, pp. 379–392.
- [20] C. DE VILLEMAGNE AND R. E. SKELTON, *Model reductions using a projection formulation*, Internat. J. Control, 46 (1987), pp. 2141–2169.
- [21] K. DECKERS, *Orthogonal Rational Functions: Quadrature, Recurrence and Rational Krylov*, PhD thesis, 2009.
- [22] V. DRUSKIN AND V. SIMONCINI, *Adaptive rational Krylov subspaces for large-scale dynamical systems*, Systems Control Lett., 60 (2011), pp. 546–560.
- [23] N. ESHGHI, T. MACH, AND L. REICHEL, *New matrix function approximations and quadrature rules based on the Arnoldi process*, J. Comput. Appl. Math., 391 (2021), pp. Paper No. 113442, 12.
- [24] S.-I. FILIP, Y. NAKATSUKASA, L. N. TREFETHEN, AND B. BECKERMANN, *Rational minimax approximation via adaptive barycentric representations*, SIAM J. Sci. Comput., 40 (2018), pp. A2427–A2455.
- [25] G. FLAGG, C. A. BEATTIE, AND S. GUGERCIN, *Interpolatory H_∞ model reduction*, Systems Control Lett., 62 (2013), pp. 567–574.
- [26] M. FRANGOS AND I. M. JAIMOUKHA, *Adaptive rational Krylov algorithms for model reduction*, in 2007 European Control Conference (ECC), 2007, pp. 4179–4186.
- [27] ———, *Adaptive rational interpolation: Arnoldi and Lanczos-like equations*, Eur. J. Control, 14 (2008), pp. 342–354.
- [28] R. W. FREUND, M. H. GUTKNECHT, AND N. M. NACHTIGAL, *An implementation of the look-ahead Lanczos algorithm for non-Hermitian matrices*, SIAM J. Sci. Comput., 14 (1993), pp. 137–158.
- [29] R. W. FREUND AND M. HOCHBRUCK, *Gauss quadratures associated with the Arnoldi process and the Lanczos algorithm*, Springer Netherlands, Dordrecht, 1993, pp. 377–380.
- [30] A. FROMMER, K. LUND, AND D. B. SZYLD, *Block krylov subspace methods for functions of matrices II: Modified block fom*, SIAM J. Matrix Anal. Appl., 41 (2020), pp. 804–837.
- [31] D. GAIER, *Lectures on complex approximation*, vol. 188, Springer, 1987.
- [32] K. GALLIVAN, A. VANDENDORPE, AND P. VAN DOOREN, *Model reduction via truncation: an interpolation point of view*, Linear Algebra Appl., 375 (2003), pp. 115–134.
- [33] ———, *Sylvester equations and projection-based model reduction*, in Proceedings of the International Conference on Linear Algebra and Arithmetic (Rabat, 2001), vol. 162, 2004, pp. 213–229.
- [34] ———, *Model reduction of MIMO systems via tangential interpolation*, SIAM J. Matrix Anal. Appl., 26 (2004/05), pp. 328–349.
- [35] G. H. GOLUB AND G. MEURANT, *Matrices, moments and quadrature with applications*, Princeton Series in Applied Mathematics, Princeton University Press, Princeton, NJ, 2010.
- [36] S. GOOSSENS AND D. ROOSE, *Ritz and harmonic Ritz values and the convergence of FOM and GMRES*, Numer. Linear Algebra Appl., 6 (1999), pp. 281–293.
- [37] K. M. GRIGORIADIS, *Optimal H_∞ model reduction via linear matrix inequalities: continuous- and discrete-time cases*, Systems Control Lett., 26 (1995), pp. 321–333.
- [38] E. GRIMME, *Krylov projection methods for model reduction*, PhD thesis, University of Illinois, 1997.
- [39] S. GUGERCIN, A. C. ANTOULAS, AND C. BEATTIE, *H_2 model reduction for large-scale linear dynamical systems*, SIAM J. Matrix Anal. Appl., 30 (2008), pp. 609–638.
- [40] S. GÜTTEL, *Rational Krylov methods for operator functions*, PhD thesis, TU Bergakademie Freiberg, Germany, 2010.
- [41] S. GÜTTEL, *Rational Krylov approximation of matrix functions: numerical methods and optimal pole selection*, GAMM-Mitt., 36 (2013), pp. 8–31.
- [42] N. J. HIGHAM, *Functions of matrices*, Society for Industrial and Applied Mathematics (SIAM), Philadelphia, PA, 2008. Theory and computation.
- [43] C. JAGELS AND L. REICHEL, *The extended Krylov subspace method and orthogonal Laurent polynomials*, Linear Algebra Appl.,

- 431 (2009), pp. 441–458.
- [44] D. KAVRANOĞLU AND M. BETTAYEB, *Characterization of the solution to the optimal H_∞ model reduction problem*, *Systems Control Lett.*, 20 (1993), pp. 99–107.
- [45] L. KNIZHNERMAN, V. DRUSKIN, AND M. ZASLAVSKY, *On optimal convergence rate of the rational Krylov subspace reduction for electromagnetic problems in unbounded domains*, *SIAM J. Numer. Anal.*, 47 (2009), pp. 953–971.
- [46] J. G. KORVINK AND E. B. RUDNYI, *Oberwolfach benchmark collection*, in *Dimension Reduction of Large-Scale Systems*, P. Benner, D. C. Sorensen, and V. Mehrmann, eds., Berlin, Heidelberg, 2005, Springer Berlin Heidelberg, pp. 311–315.
- [47] E. LEVIN AND E. B. SAFF, *Potential theoretic tools in polynomial and rational approximation*, in *Harmonic analysis and rational approximation*, vol. 327 of *Lect. Notes Control Inf. Sci.*, Springer, Berlin, 2006, pp. 71–94.
- [48] J.-R. LI AND J. WHITE, *Low rank solution of Lyapunov equations*, *SIAM J. Matrix Anal. Appl.*, 24 (2002), pp. 260–280.
- [49] R.-C. LI AND Z. BAI, *Structure-preserving model reduction using a Krylov subspace projection formulation*, *Commun. Math. Sci.*, 3 (2005), pp. 179–199.
- [50] J. LIESEN AND Z. STRAKOŠ, *Krylov subspace methods: principles and analysis*, *Numerical Mathematics and Scientific Computation*, Oxford University Press, Oxford, 2013.
- [51] Y. LIN, *Transfer function interpolation remainder formula of rational krylov subspace methods*, arXiv manuscript, (2021).
- [52] Y. LIN AND V. SIMONCINI, *Minimal residual methods for large scale Lyapunov equations*, *Appl. Numer. Math.*, 72 (2013), pp. 52–71.
- [53] ———, *A new subspace iteration method for the algebraic Riccati equation*, *Numer. Linear Algebra Appl.*, 22 (2015), pp. 26–47.
- [54] Y. LIN, X. WANG, AND L.-H. ZHANG, *Solving symmetric and positive definite second-order cone linear complementarity problem by a rational Krylov subspace method*, *Appl. Numer. Math.*, 176 (2022), pp. 104–117.
- [55] G. LÓPEZ LAGOMASINO, L. REICHEL, AND L. WUNDERLICH, *Matrices, moments, and rational quadrature*, *Linear Algebra Appl.*, 429 (2008), pp. 2540–2554.
- [56] V. MEHRMANN AND T. STYKEL, *Balanced truncation model reduction for large-scale systems in descriptor form*, in *Dimension reduction of large-scale systems*, vol. 45 of *Lect. Notes Comput. Sci. Eng.*, Springer, Berlin, 2005, pp. 83–115.
- [57] B. C. MOORE, *Principal component analysis in linear systems: controllability, observability, and model reduction*, *IEEE Trans. Automat. Control*, 26 (1981), pp. 17–32.
- [58] C. T. MULLIS AND R. A. ROBERTS, *Synthesis of minimum roundoff noise fixed point digital filters*, *IEEE Trans. Circuits and Systems, CAS-2* (1976), pp. 551–562.
- [59] Y. NAKATSUKASA, O. SÈTE, AND L. N. TREFETHEN, *The AAA algorithm for rational approximation*, *SIAM J. Sci. Comput.*, 40 (2018), pp. A1494–A1522.
- [60] R. F. P. FELDMANN, *Reduced-order modeling of large linear subcircuits via a block lanczos algorithm*, in *32nd Design Automation Conference*, 1995, pp. 474–479.
- [61] C. C. PAIGE, B. N. PARLETT, AND H. A. VAN DER VORST, *Approximate solutions and eigenvalue bounds from Krylov subspaces*, *Numer. Linear Algebra Appl.*, 2 (1995), pp. 115–133.
- [62] H. K. F. PANZER, *Model Order Reduction by Krylov Subspace Methods with Global Error Bounds and Automatic Choice of Parameters*, PhD thesis, 2014.
- [63] S. POZZA AND M. PRANIĆ, *The Gauss quadrature for general linear functionals, Lanczos algorithm, and minimal partial realization*, *Numer. Algorithms*, 88 (2021), pp. 647–678.
- [64] S. POZZA, M. S. PRANIĆ, AND Z. STRAKOŠ, *Gauss quadrature for quasi-definite linear functionals*, *IMA J. Numer. Anal.*, 37 (2017), pp. 1468–1495.
- [65] ———, *The Lanczos algorithm and complex Gauss quadrature*, *Electron. Trans. Numer. Anal.*, 50 (2018), pp. 1–19.
- [66] S. POZZA AND Z. STRAKOŠ, *Algebraic description of the finite Stieltjes moment problem*, *Linear Algebra Appl.*, 561 (2019), pp. 207–227.
- [67] Y. SAAD, *Iterative methods for sparse linear systems*, *Society for Industrial and Applied Mathematics*, Philadelphia, PA, second ed., 2003.
- [68] W. H. A. SCHILDERS, H. A. VAN DER VORST, AND J. ROMMES, eds., *Model order reduction: theory, research aspects and applications*, vol. 13 of *Mathematics in Industry*, Springer-Verlag, Berlin, 2008. European Consortium for Mathematics in Industry (Berlin).
- [69] M. SCHWEITZER, *A two-sided short-recurrence extended Krylov subspace method for nonsymmetric matrices and its relation to rational moment matching*, *Numer. Algorithms*, 76 (2017), pp. 1–31.
- [70] V. SIMONCINI, *A new iterative method for solving large-scale Lyapunov matrix equations*, *SIAM J. Sci. Comput.*, 29 (2007), pp. 1268–1288.
- [71] ———, *Analysis of the rational Krylov subspace projection method for large-scale algebraic Riccati equations*, *SIAM J. Matrix Anal. Appl.*, 37 (2016), pp. 1655–1674.
- [72] Z. STRAKOŠ, *Model reduction using the Vorobyev moment problem*, *Numer. Algorithms*, 51 (2009), pp. 363–379.
- [73] N. VAN BUGGENHOUT, M. VAN BAREL, AND R. VANDEBRIL, *Biorthogonal rational Krylov subspace methods*, *Electron. Trans. Numer. Anal.*, 51 (2019), pp. 451–468.
- [74] A. YOUSUFF AND R. E. SKELTON, *Covariance equivalent realizations with application to model reduction of large-scale systems*, in *Control and dynamic systems*, Vol. 22, Academic Press, Orlando, FL, 1985, pp. 273–348.
- [75] A. YOUSUFF, D. A. WAGIE, AND R. E. SKELTON, *Linear system approximation via covariance equivalent realizations*, *J. Math. Anal. Appl.*, 106 (1985), pp. 91–115.